ARL-TR-9503 ● JULY 2022

DEVCOM ARMY RESEARCH LABORATORY

Novel Methodologies for Multiscale Modeling of Army Materials (Summary Technical Report, 2011–2021)

by Jaroslaw Knap, Kenneth W Leiter, Joshua C Crone, William D Mattson, Betsy M Rice, Berend C Rinderspacher, and Oleg Borodin

NOTICES

Disclaimers

The findings in this report are not to be construed as an official Department of the Army position unless so designated by other authorized documents.

Citation of manufacturer's or trade names does not constitute an official endorsement or approval of the use thereof.

Destroy this report when it is no longer needed. Do not return it to the originator.

ARL-TR-9503 ● JULY 2022

Novel Methodologies for Multiscale Modeling of Army Materials (Summary Technical Report, 2011–2021)

Jaroslaw Knap, Kenneth W Leiter, Joshua C Crone, William D Mattson, Betsy M Rice, Berend C Rinderspacher, and Oleg Borodin
DEVCOM Army Research Laboratory

REPORT DOCUMENTATION PAGE

Form Approved
OMB No. 0704-0188

1. REPORT DATE *(DD-MM-YYYY)*	2. REPORT TYPE	3. DATES COVERED (From - To)
July 2022	Summary Technical Report	2011–2021

4. TITLE AND SUBTITLE
Novel Methodologies for Multiscale Modeling of Army Materials (Summary Technical Report, 2011–2021)

5a. CONTRACT NUMBER

5b. GRANT NUMBER

5c. PROGRAM ELEMENT NUMBER
611102.AA7.13

6. AUTHOR(S)
Jaroslaw Knap, Kenneth W Leiter, Joshua C Crone, William D Mattson, Betsy M Rice, Berend C Rinderspacher, and Oleg Borodin

5d. PROJECT NUMBER

5e. TASK NUMBER

5f. WORK UNIT NUMBER

7. PERFORMING ORGANIZATION NAME(S) AND ADDRESS(ES)
DEVCOM Army Research Laboratory
ATTN: FCDD-RLC-EM
Aberdeen Proving Ground, MD 21005

8. PERFORMING ORGANIZATION REPORT NUMBER
ARL-TR-9503

9. SPONSORING/MONITORING AGENCY NAME(S) AND ADDRESS(ES)

10. SPONSOR/MONITOR'S ACRONYM(S)

11. SPONSOR/MONITOR'S REPORT NUMBER(S)

12. DISTRIBUTION/AVAILABILITY STATEMENT
Approved for public release: distribution unlimited.

13. SUPPLEMENTARY NOTES
ORCID IDs: Joshua C Crone, 0000-0003-0856-9149; Betsy M Rice, 0000-0002-8221-0356; Berend C Rinderspacher, 0000-0003-1333-1653; and Oleg Borodin, 0000-0002-9428-5291

14. ABSTRACT
The objectives of the US Army Combat Capabilities Development Command Army Research Laboratory's cross-cutting effort, Enterprise for Multiscale Research of Materials (PE 611102.AA7.13 "Multiscale Modeling for Novel Materials"), were to explore and develop multiscale modeling techniques to support fundamental studies of electronic and structural material properties from the atomistic to the continuum. The resulting models were created to design and develop materials for more-efficient, longer-lifetime sensors and power and energy devices, and lighter materials for vehicle and Soldier protection. This effort includes coupled research with two 5-year Collaborative Research Alliances (CRAs): the Materials in Extreme Dynamic Environments CRA and the Multi-Scale/Multidisciplinary Modeling of Electronic Materials CRA (PE 611104.AB7.09 "Multiscale Modeling of Materials Center").

15. SUBJECT TERMS
Network and Computational Sciences, Sciences of Extreme Materials, Weapons Sciences, multiscale modeling, materials science, computational science, scale-bridging, density functional theory, dislocation dynamics

16. SECURITY CLASSIFICATION OF:			17. LIMITATION OF ABSTRACT	18. NUMBER OF PAGES	19a. NAME OF RESPONSIBLE PERSON
a. REPORT	b. ABSTRACT	c. THIS PAGE			Jaroslaw Knap
Unclassified	Unclassified	Unclassified	UU	62	19b. TELEPHONE NUMBER (Include area code) (410) 278-0420

Contents

List of Figures

Executive Summary

The ability to rapidly design materials specifically tailored to particular applications hinges on the use of predictive material models. Over the last few decades, multiscale modeling has emerged as the leading paradigm for constructing material models. This report summarizes efforts toward development of methodologies in multiscale modeling carried out as part of the US Army Combat Capabilities Development Command Army Research Laboratory's cross-cutting effort, Enterprise for Multiscale Research of Materials spanning 2011 to 2021 (PE 611102.AA7.13 "Multiscale Modeling for Novel Materials"). This effort included coupled research with two 5-year Collaborative Research Alliances (CRAs): the Materials in Extreme Dynamic Environments CRA and the Multi-Scale/Multidisciplinary Modeling of Electronic Materials CRA (PE 611104.AB7.09 "Multiscale Modeling of Materials Center").

Three research thrusts constituted the overall effort. The overarching goal of the first research thrust was to construct computational methodologies to facilitate data transfers between at-scale models in a multiscale model hierarchy to allow construction of multiscale models by directly linking at-scale models. A major contribution of this thrust was development of a flexible modular software environment for scale bridging.

The second thrust focused on developing new approaches to enable a first-principles exploration of the relationship between the atomic-scale structural features of real materials and their macroscopic properties. The thrust yielded significant enhancements of a leading large-scale first-principles software suite to substantially reduce computational requirements for condensed phase systems, while extending the functionality of the package to address Army problems.

Finally, the third thrust was dedicated to new methodologies for mesoscale modeling of small-scale plasticity, the motion of dislocations within materials. The thrust led to development of a unique computational capability allowing us to fuse state-of-the-art computational models of small-scale plasticity with finite elements. This capability permits accurate modeling of small-scale plasticity in the presence of microstructure.

1. Introduction

Our ability to rapidly design materials specifically tailored to applications rests on predictive material models. Such models allow us to establish direct linkages between material structure, processing, and performance. Over the last few decades, multiscale modeling has emerged as the leading paradigm for developing high-fidelity material models. In multiscale modeling, one starts by identifying the relevant scales (spatial and temporal) along with the dominant phenomena operating at these scales; then, at-scale models of these phenomena are constructed; and finally, at-scale models are combined into a single multiscale model.

The focus of the US Army Combat Capabilities Development Command (DEVCOM) Army Research Laboratory's cross-cutting effort, Enterprise for Multiscale Research of Materials (EMRM), spanning 2011 to 2021, was on research toward developing novel methodologies in multiscale modeling (PE 611102.AA7.13 "Multiscale Modeling for Novel Materials"). The effort included coupled research with two 5-year Collaborative Research Alliances (CRAs): the Materials in Extreme Dynamic Environments CRA and the Multi-scale/Multidisciplinary Modeling of Electronic Materials CRA (PE 611104.AB7.09 "Multiscale Modeling of Materials Center"). Three specific research thrusts were pursued: one dedicated to methodologies for bridging scales and two devoted to crucially important at-scale models.

The overarching goal of the first thrust was to construct methodologies (numerical methods and algorithms) to facilitate data exchanges between at-scale models in a multiscale model hierarchy. At the onset of the project, it was recognized that the advent of peta- and exa-scale computing offered new opportunities to allow construction of multiscale models by directly linking at-scale models. Yet, at the time, few tools and software libraries existed to enable seamless data exchanges between at-scale models, especially on extreme-scale computers. In addition, it was recognized that such tools and libraries were crucial as enabling technologies in multiscale modeling. A major contribution of the first research thrust was development of a flexible modular software environment for scale bridging called the hierarchical multiscale simulation (HMS).

The focus of the second thrust was on developing new approaches to enable a first-principles exploration of the relationship between the atomic-scale structural features of real materials and their macroscopic properties. At the time of the inception of the project, current capabilities in quantum mechanics (QM) precluded real material solutions. Novel order reduction and next-generation computational physics algorithms were needed to expand exploration of material science problems

using QM approaches. The QM thrust yielded significant enhancements of a leading large-scale density functional theory (DFT) software suite that substantially reduced the computational requirements for condensed phase systems while extending the functionality of the package to address Army problems. This included an ability to provide a first-ever QM description of local stress in a material, and a capability to calculate accurate electron transport for systems with interfaces and defects.

Finally, the third thrust was dedicated to new methodologies for mesoscale modeling of small-scale plasticity. Small-scale plasticity, the motion of dislocations within materials, affects many properties, such as strength or ductility. Small-scale plasticity is to a large extent affected by the presence of various microstructural features. Yet, at the beginning of the cross-cutting effort, existing approaches, such as molecular dynamics (MD) or crystal plasticity, were considered not particularly well suited to handle all the length scales involved. Hence, new approaches, capable of dealing with the discrete nature of dislocations on one hand and of attaining proper continuum limits on the other, were needed. The third thrust led to development of a computational capability that allows seamless and efficient fusion of state-of-the-art (SOA) computational models of small-scale plasticity with finite elements (FEs). Such a capability is truly unique and enables accurate modeling of small-scale plasticity in the presence of microstructure.

These three thrusts are described in detail in subsequent sections.

2. Methodologies for Scale Bridging in Multiscale Simulation

The goal of materials design is to create new materials with desired properties and functionality. The successful application of a materials design concept requires the existence of high-fidelity material models. A material model is a logical description of material behavior in an external environment. Typically, two material model classes are considered: empirical and theory-based. An empirical material model directly incorporates experimental observations by means of fitting them to certain mathematical expressions. Therefore, an empirical model is typically valid only within a small range of parameters and environmental conditions covered by the experiments on which it has been developed. Moreover, any extrapolation outside that range can lead to great uncertainties as confidence intervals are notoriously difficult to calculate. In contrast, a theory-based model is built upon fundamental principles developed within or across scientific disciplines (mechanics, physics, chemistry, etc.). Owing to its multi-science origins, the theory-based model allows us to sidestep the trial-and-error character of the empirical model leading to a

deeper understanding of a material's behavior. For these reasons, theory-based models are expected to have better predictive character.

In the last few decades, combined theoretical, computational, and experimental efforts have led to emergence of a new class of material models: multiscale. The concept of a multiscale model is an extension of the theory-based model and aims to systematically analyze the material behavior from the viewpoint of all spatial and temporal scales controlling it. In the context of multiscale material models, computation plays a crucial role as a primary driver for innovation. Harnessing the power of high-performance computing (HPC), in particular peta- or exa-scale computing, for materials modeling is likely to lead to significant advances in both fidelity and speed of predictions. However, HPC requires not only science-based models, but also novel numerical methods and algorithms, in particular, numerical methods and algorithms for multiscale modeling capable of scalable and adaptive computation on emerging high-performance computers.

Prior to the DEVCOM Army Research Laboratory (ARL) research effort summarized in this report, no general numerical and computational framework existed for development of hierarchical (sequential and concurrent) multiscale models on peta- and exa-scale computing environments. Most of the scale bridging necessary to develop multiscale models was carried out "by hand" on a case-by-case basis, offering little to no reuse between models, and few algorithms were available to speed development of scale bridging for multiscale models. During the research effort, a review article on the current state of available multiscale computing software was authored with European colleagues and described the critical need for software and tools to aid development and evaluation of multiscale models on emerging HPC architectures (Groen et al. 2019). The report concluded that current tools for multiscale modeling were still quite immature, and algorithms and software for multiscale modeling were in great need of development.

The goal of the research effort was to develop an adaptive numerical and computational software environment for hierarchical (sequential and concurrent) multiscale modeling on peta- and exa-scale computing environments, specifically parallel, hybrid, and distributed systems. To achieve the goal, the effort consisted of three complementary efforts: 1) development of adaptive algorithms to quickly combine both new and existing at-scale models together to form a multiscale model, 2) development of algorithms for spatial and temporal scale bridging, and 3) development of algorithms for surrogate modeling to expedite multiscale model evaluation. These research efforts were envisioned to be broadly applicable to many materials applications of interest to the Army. Throughout the research project, developed algorithms were applied to and evaluated in the context of Army-

relevant materials modeling applications, including composite materials, energetic materials, and electrochemistry.

A major contribution of the research effort was development of a flexible modular software environment for scale bridging, the HMS software (Knap et al. 2016). The HMS scale-bridging software applies an adaptive computational approach to combine both newly developed and existing at-scale models to form multiscale models well suited for evaluation on large-scale heterogeneous HPC systems. Each at-scale model resolves the processes at a single spatial and/or temporal scale relevant to the overall behavior of the system. The HMS software views a multiscale model as a collection of two-scale model building blocks. Each two-scale model building block consists of an upper scale model (macroscale) and lower scale (microscale) model. The upper scale model acquires missing quantities through direct evaluation of the lower scale model. Following its evaluation, required data is extracted from the lower scale model to inform the upper scale model. By combining the two-scale model building blocks together, the HMS software is capable of modeling a wide variety of multiscale systems.

As a first demonstration of the HMS software, a multiscale model of a composite material was developed that consisted of a FE upper scale model of a deforming body and a FE lower scale model of a composite fiber and matrix. The lower scale model computed the average Cauchy stress given the deformation gradient provided by the upper scale model. A simulation of a Taylor-impact experiment of a composite cylinder impacting a rigid anvil was performed that required over a billion lower scale model evaluations, demonstrating the ability of the HMS software to efficiently coordinate interactions between the individual models. One challenge encountered with the multiscale model was that for large deformations, the evaluation time of the lower scale model was greater than for small deformations, leading to a load imbalance among the processors. To address the issue, a round-robin load balancing algorithm was developed in the HMS software and was shown to reduce the overall evaluation time of the multiscale model by more than 50%.

An important material system to the Army that motivated much of the development of the HMS software and scale-bridging algorithms was energetic materials (EMs). EMs are particularly difficult to model due to their intricate molecular structure and heterogeneous composition. Many energetic formulations consist of crystalline grains of EMs embedded in a polymer matrix, where microstructural heterogeneities, such as inter- and intragranular voids, grain sizes, grain orientations, and grain compositions dictate their macroscale properties and explosive response to external stimuli. When subjected to thermal or mechanical loading, energy localization at stress concentrators at pores or other material defects

initiates chemical reactivity that may ultimately lead to deflagration, detonation, or damage of EMs. Although chemical decomposition and energy release occur at the molecular scale, they are tightly coupled to the material properties and explosive response observed at the macroscale. Widely used molecular-based methods including MD and dissipative particle dynamics are restricted to modeling the EM behavior at short timescales and in relatively small volumes. On the other hand, continuum models are able to model the shock and detonation response of EMs at length and timescales relevant to system-level applications. However, continuum models developed to date require extensive fitting to material data acquired from experiments to make accurate predictions and therefore have limited transferability to conditions beyond the scope of the experimental data. Multiscale models of EMs that resolve relevant processes at their appropriate scales, such as chemical decomposition, pore collapse, and grain-scale interactions, promise to provide greater predictive ability, reduce or eliminate reliance on expensive and dangerous methods to acquire experimental data, and facilitate the design of new energetics formulations that have desired properties.

An initial proof-of-concept multiscale model of the EM 1,3,5-*s*-triazine (RDX) has been developed using the HMS scale-bridging approach (Leiter et al. 2018). The multiscale model consists of two at-scale models: an upper scale continuum FE model of a deforming body implemented in ALE3D and a lower scale dissipative particle dynamics model implemented in the Large-scale Atomic/Molecular Massively Parallel Simulator (LAMMPS) (Thompson et al. 2022). In the model, the equation of state (EOS) of RDX utilized in the upper scale model is directly obtained from evaluation of the lower scale model. A Python package to automate evaluation of the EOS using LAMMPS has been developed (Barnes et al. 2017). The EOS is obtained from the dissipative particle dynamics model for every FE at every timestep of the upper scale model. A Taylor impact simulation has been performed using the developed multiscale model and despite the FE model only containing 1600 FEs, the entire model required nearly ten million CPU hours to evaluate, clearly making the multiscale model impractical for routine use.

To reduce computational cost, a standalone module has been developed in the HMS software responsible for surrogate modeling. The surrogate modeling approach used in the HMS software is adapted from the Adaptive Sampling methodology at the Lawrence Livermore National Laboratory (LLNL) (Knap et al. 2008). In the HMS surrogate modeling module, data acquired from the microscale model during its evaluation is stored in a database and used to construct surrogate models during the multiscale model evaluation. When a new microscale model evaluation is required, the HMS software determines whether an existing surrogate model can be used to perform the evaluation in lieu of the microscale model on the basis of an

error estimate. When the error estimate is below a user-defined threshold, the surrogate model is evaluated rather than the microscale model, greatly reducing the computational cost. In the case where the microscale model must be evaluated, the obtained result is stored in the database and used to update the surrogate model so as the multiscale model evaluation proceeds, the surrogate model increases accuracy and learns the microscale model response across the input ranges relevant to the upper scale model. Using the developed surrogate modeling approach, the overall computational cost of the RDX multiscale model is shown to be 1/20 to 1/5000 of the original computational cost, depending on the desired accuracy. Furthermore, the overall error in the solution is controllable.

One challenge of the surrogate modeling approach is that it increases the computational variability in the simulation. It is difficult to predict a priori how often the surrogate model or the microscale model will be evaluated, making it difficult to efficiently assign computational resources to the simulation. At times, this can lead to idle processors that wait for lower scale model evaluations to complete. Barnes et al. (2020) explored the use of speculative microscale model evaluations in the HMS software to utilize idle processors present in a multiscale simulation. The use of speculative evaluations was shown to further reduce the overall time required to perform the multiscale simulation. Further work in Barnes et al. (2020) explored modeling voids in the microscale model and their impact on the computed EOS.

The initial multiscale model of RDX summarized previously did not consider chemistry, even though decomposition of RDX into product gases is a fundamental process leading to its explosive properties. To incorporate chemistry into multiscale models of EMs, temporal scale-bridging methodologies for chemistry have been developed (Leiter et al. 2022) and applied to multiscale modeling of RDX. In the multiscale modeling literature, methodologies for temporal scale bridging are lacking in comparison to methodologies for spatial scale bridging, an indicator that temporal scale bridging is a significantly more difficult problem.

To handle chemistry in the multiscale model of RDX, two lower scale models are utilized, one to evaluate the EOS and another to compute the instantaneous rates of chemical decomposition. Both lower scale models are based on the newly developed reactive dissipative particle dynamics (DPD-RX) method (Lísal et al. 2019). In the upper scale model, a postulated model of RDX chemistry is formulated, described by a coupled system of ordinary differential equations that contain unknown reaction rate coefficients. The unknown reaction rate coefficients of the upper scale chemistry model are estimated from the rates of decomposition acquired from the lower scale model. Using the estimated reaction rate coefficients,

the upper scale model is able to evolve its chemistry over the timestep, which is orders of magnitude greater than the timestep of the lower scale model.

Several simulations have been performed to assess the capability of the model, including simulation of a scaled thermal explosion experiment (STEX). The STEX experiment is a carefully constructed experiment used to validate models of EMs and consists of an EM confined within a cylindrical steel vessel that is slowly heated until the EM undergoes chemical decomposition. In simulations of the STEX experiment, the multiscale model can initiate chemical decomposition of RDX leading to high temperature and pressure states. A comparison of hoop strain measurements in the simulation compared to previously published literature of RDX-based explosives shows qualitative agreement indicating that the model does well in capturing the general material response. Overall, the temporal scale-bridging methodology is shown to capture the strong coupling between chemical decomposition and provides evidence that the requisite spectrum of material response may be achievable with these scale-bridging algorithms.

The most recent work on multiscale modeling of energetics is focused on applying the multiscale model to applications of interest to the energetics community, especially to plate impact simulations to obtain Pop plots that measure run distance to detonation. A major challenge is the extreme computational cost of the multiscale model. New methodologies for surrogate modeling of chemistry are required to reduce the computational cost. Such surrogate models are fundamentally different than those developed so far (i.e., for the EOS) as they must capture the temporal evolution of chemistry and ensure that physical constraints, such as mass balance, are satisfied. More developments are also needed for both spatial and temporal scale bridging of relevant microstructure in EMs, such as pores.

The HMS approach to multiscale model development also has relevance to other materials science applications outside of multiscale modeling. For example, high-throughput applications for discovery of materials are well suited to the distributed and adaptive mode of computation that the HMS software provides. To this end, the HMS software has been augmented with a specialized module to route individual model evaluations to nonlocal computational resources and a high-throughput application has been created using the HMS software to discover candidate electrolytes for batteries (Borodin et al. 2015, 2015d; Knap et al. 2015). In the high-throughput application, a discovery algorithm searches for battery electrolyte solvents with desired electrochemical stability through analysis of their first and second reduction and oxidation potentials. A screening algorithm dynamically evaluates parallel DFT calculations on available remote computational resources. The DFT calculations either perform an initial geometry optimization or compute the oxidation and reduction potentials under two different fidelities,

depending on the requirements of the screening application. The HMS software was shown to successfully coordinate the high-throughput screening, restart model evaluations that failed over the course of the screening, and schedule DFT evaluations adaptively based on the current computational load at the nonlocal resources.

The uncertainty quantification of multiscale models is necessary for robust design optimization of multiscale systems and understanding the variability of system performance across the range of uncertain inputs. Traditional uncertainty quantification methods, such as Monte Carlo, polynomial chaos, and stochastic collocation, require repeated sampling of a model under consideration given different realizations of the random variables. Repeated sampling of multiscale models is often impossible as a single model evaluation is already extremely computationally demanding. New methods for uncertainty quantification specifically tailored to multiscale models are needed.

For multiscale models, one particular problem of interest is uncertainty quantification of an individual at-scale model within the multiscale model hierarchy. One motivating example to consider is an at-scale model that incorporates microstructure, such as porosity. A probabilistic description of the microstructure can be formulated, for example, a distribution of pore sizes and shapes that leads to a distribution of model responses. To facilitate this type of uncertainty quantification in multiscale models, the HMS scale-bridging software has been extended to incorporate the UQPy uncertainty quantification package (Olivier et al. 2020) from the Johns Hopkins University. UQPy implements many SOA uncertainty quantification algorithms to compute distributions of model responses. Python language bindings to HMS have been developed to enable the use of Python packages, such as UQPy, directly in the HMS software framework. A simple example problem of Monte Carlo integration using HMS and UQPy was developed, and further work is ongoing to use the methodology for a model of porosity in magnesium (Mg). In the future, the HMS Python bindings can be used to incorporate widely used machine learning (ML) packages into the HMS software to facilitate surrogate model development. Furthermore, the HMS Python bindings allow for development of HMS-based multiscale models in Python, enabling quick multiscale model prototyping and development.

The HMS scale-bridging software has been designed to allow for use of any existing at-scale model within a multiscale model hierarchy. When the at-scale model is used as the lower scale model, no software modifications to the model are required, which allows for the use of closed-source or proprietary software packages. However, when the at-scale model is used as an upper scale model in a multiscale model hierarchy, software modifications have traditionally been

required to utilize the HMS software. For example, to develop the RDX model discussed previously, a customized material model was implemented within ALE3D. To avoid the requirement to modify the source code of upper scale models, which are often complex and closed-source, recently a vectorized user material (VUMAT) model for HMS has been developed, named the HMS-VUMAT. VUMAT is a standardized custom material model application programming interface implemented in a number of widely used industry and government FE codes, including ALE3D, EPIC, Sierra, ALEGRA, ABAQUS, and LS-DYNA. The HMS-VUMAT allows for the implementation of HMS-based multiscale models in any software that supports the VUMAT standard without source code modification, and HMS-VUMAT models can be easily moved between any of the VUMAT-supported codes. The ultimate goal is to make the HMS-VUMAT a widely used standard for multiscale model development in FE software.

To summarize, the research effort on methodologies for scale bridging in multiscale simulation focused on developing computational methods and algorithms to enable efficient creation and evaluation of multiscale models on emerging HPC architectures. The effort resulted in the creation of the HMS scale-bridging software, which establishes an adaptive computational approach to multiscale model development and incorporates advanced surrogate modeling methodologies to ensure that the models have tractable computational cost. Several algorithms for both spatial and temporal scale bridging of microstructure and chemistry in materials have been developed. The scale-bridging approaches were evaluated in the context of several materials systems important to the Army, including composites, EMs, and metals. Still, much work on computational methodologies for multiscale modeling remains, including surrogate modeling in high dimensions, surrogate modeling to handle the temporal evolution of chemistry and microstructure, surrogate modeling tailored to physical systems, uncertainty quantification for multiscale models, and further maturation of the methodologies developed in this effort and their incorporation into widely used DOD modeling codes.

3. Quantum Mechanics for Material Science

The SOA for full-resolution quantum mechanical treatment of condensed phase materials was (and still is) O(N) DFT. Traditional DFT methods scale as the cube of the number of electrons (i.e., $O(N^3)$]. O(N) methods attempt to reduce the order to a theoretical minimum of linear scaling. Historically, the main obstacle to the implementation of O(N) methods has been the system size required to see these methods outperform traditional methods, often requiring system sizes of tens of thousands of atoms to see improved performance over traditional methods. Recent

advances in both algorithms and hardware have made O(N) methods more feasible as we are simulating system sizes in that larger regime and algorithmic development has reduced the cross-over point in systems comprising a few thousand atoms. Furthermore, the O(N) methods have traditionally relied on electron localization to achieve its reduced scaling. The degree of conductivity of a material is inversely proportional to the electron localization of the material. Molecular systems naturally have localized electrons (i.e., are insulators) and are good targets for traditional O(N) methods. However, metals and other conducting materials do not have localized electrons and are a challenge for O(N) methods. This is a particular difficulty for the goals of the overall Quantum Mechanics for Material Science (QMMS) program, which is to provide large-scale DFT simulation capabilities for materials of Army interest, among which metals and conducting materials play an important role.

After surveying SOA "large-scale" DFT codes, we found that the CP2K suite (Kuhne et al. 2020) had the best mix of O(N) methodologies and functionality, although the feature sets in CP2K were not as extensive as those of SOA small-scale DFT codes such as the Vienna Ab initio Simulation Package (VASP) (Kresse and Furthmüller 1996). CP2K uses localized Gaussian orbitals augmented with plane waves and other basis sets and has demonstrated the capability to simulate thousands of atoms for picoseconds with HPC resources. CP2K is licensed under GNU General Public License and invites contributors to its further development. CP2K has been used to perform accurate Kohn–Sham (KS) DFT calculations for approximately 1,000,000 atoms in limited situations (e.g., a few single-point energies, low valence electron count). The more realistic "large-scale" practical KS-DFT calculations (e.g., Born–Oppenheimer molecular dynamics [BOMD]) for systems containing heavy atoms are limited to approximately 10,000 atoms; our goals were to go well beyond this. Our strategy to extend timescale and size of relevant simulations was to augment the CP2K program package to dramatically reduce memory requirements per node using distributed data types, reduce costs of sparse matrix multiplies, and provide more-efficient energy minimization algorithms.

Even with such improvements to CP2K to enable routine simulations of systems composed of 1,000,000 atoms, the system size is too small to allow adequate depictions of important microstructural material features, such as extended defects, interfaces, or dopants. The depiction of these complex material features at the atomistic scale requires special treatment of boundary conditions in the calculations to mimic larger sizes. The SOA for treatment of unusual boundary conditions include coarse-grained DFT, Exactly Embedded (EE)-DFT, and Green's functions methods. However, at the beginning of the project, those methods were in their

infancy and implementation into highly scalable software was in its initial stages. Therefore, within this effort, we explored emerging multi-resolution DFT approaches, including EE-DFT and quasi-continuum DFT (QC-DFT), to determine their viability for problems of Army interest.

Finally, to ensure the usefulness of the proposed implementations, they were validated against calculations using existing codes as well as experiments for calculations beyond the scope of the scale of existing codes.

3.1 Full-Resolution DFT

3.1.1 Software Improvement

Determining the electronic structure in a system is accomplished by minimizing its energy with respect to the distribution of the electrons (i.e., the electron density). Within this minimization, sparse matrices are prepared and used in a number of different ways. The number of sparse matrix multiplies required to obtain the energy minimum are dependent a number of factors. To accommodate the larger simulations required to treat systems of interest to the Army, CP2K required improvements in minimization algorithms and reduced memory requirements. To this end, we undertook several activities to improve minimization or reduce memory requirements. One activity (the implementation of the second-order trace conserving [TC2] method detailed next) accomplished both.

We implemented methods to improve the efficiency of the energy minimization by including density matrix purification methods. As stated in Mullin (2014), "Purification is analogous to preconditioning in linear algebra, but the transformation is intended to resolve the Kohn–Sham matrix such that it becomes idempotent. This relies on predefined polynomials, which must balance the order of the polynomial with the number of iterations needed to create an idempotent matrix." At the beginning of the project, CP2K utilized the fourth-order trace resetting (TRS4) method to monotonically transform the KS matrix to idempotency. A fourth-order method requires CP2K to maintain four sparse matrices for the method. We implemented a nonmonotonic approach proposed to treat low-bandgap systems, the TC2 method, which only requires CP2K to maintain two sparse matrices. This method weights a second-order polynomial based on the highest occupied molecular orbital (HOMO) and lowest unoccupied molecular orbital (LUMO) energies for use in transforming the KS matrix to idempotency. The reduced degree of polynomial used in TC2 compared to the fourth-order polynomial used in TRS4 reduces the memory requirements by half and reduces the number of matrix-matrix multiplications. Implementation of TC2 in CP2K allowed for a calculation of a single MD step for a system of 100,000 atoms. Using

the same resources, the largest system that could be calculated with TRS4 was 50,000 atoms. Furthermore, we found that the TC2 method improved performance for materials with lower resistance to conductivity (i.e., with electrons that are less localized), but still does not work for metallic systems (full electron delocalization). Note some systems have a short-range conductivity (e.g., a shock front in an energetic molecular crystal) and TC2 will work better than TRS4 for those systems.

We also implemented a method proposed by Suryanarayana (2013) that claimed to allow O(N) methods to function for conductive materials. The test system that he demonstrated in his paper was idealized and we found that in real systems of interest to the Army, the method did not improve upon the TC2 method.

Reduced memory footprint: CP2K previously had a large amount of replicated data, which significantly expands the memory footprint, thus limiting the possible simulation size and the scalability of the software package. We updated and tested the hybrid OpenMP/MPI implementation to reduce the frequency of data replication. We further reduced the memory footprint by modifying the replicated data structures and their communication protocols so that they are distributed as needed across the simulation. Furthermore, the TC2 linear-scaling method that we implemented reduces the memory requirement by 33% for large systems.

Optimizing the sparse matrix multiply: Sparse matrix multiplies account for at least 95% of the computational time for large systems. Developing algorithms for ever-more-efficient sparse matrix multiplies has been of considerable interest for decades; however, there is no unique solution, as the efficiency is dependent on basis set and the physics of the problem. CP2K has a very efficient Gaussian-augmented plane-wave basis set that gives fairly good spatial localization of the electrons; however, the plane-wave augmentation tends to make the sparsity more diffuse than a strictly Gaussian basis would. The implementation of the sparse-matrix multiplies in CP2K is not optimal for this basis set; thus, we implemented a more efficient methodology for sparse matrix multiplies. Specifically, we implemented a hypergrid communication pattern to replace the Cartesian grid pattern currently used (leftmost frame of Fig. 1) to reduce the cost of the sparse matrix multiply. The rightmost frame of Fig. 1 shows a resulting communication grid based on the new method. It is clear that the new method provides a pattern that is more localized, thus reducing communication (number of MPI calls), and therefore more efficient for sparse-matrix multiplies.

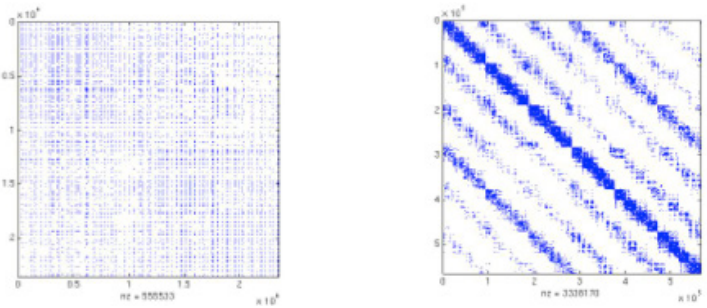

Fig. 1 Communication grids for Gaussian-augmented plane-wave basis in CP2K, with process numbers along the axes. A color in any element indicates communication between the two processes. (Left) Example of the original Cartesian communication pattern. (Right) Example of a modified communication pattern.

Optimizing the calculation of the density: Direct Inversion in the Iterative Subspace (DIIS) (Pulay 1980, 1982) is a method that reduces the number of sparse matrix multiplies per self-consistent cycles required to obtain the density. DIIS was implemented for the $O(N^3)$ methods in CP2K, but not for the linear-scaling methods. We adapted the DIIS method for use with linear scaling, first for the TRS4 algorithm already implemented in CP2K and then for the TC2 algorithm that we implemented into CP2K.

We also implemented the Krylov Subspace Accelerated Inexact Newton (KAIN) method (Harrison 2004) for solving a multiple linear equation in the O(N) version of CP2K and compared with the optimized DIIS method. The KAIN method did not outperform the optimized DIIS and was not further pursued.

Further improvement was obtained through modifying the initial guess of the density matrix, which originally used the sum of isolated atomic densities. Such initial guesses show difficulty in convergence for bonded systems due to the "empty" density space between the atoms. To overcome this, we added random fluctuations to the initial guess (i.e., into the "empty" density space between the atoms). This allowed the methods for calculating the density to more rapidly converge to the correct density in those empty spaces, thus reducing the number of sparse matrix multiplies needed.

3.1.2 Enhanced Functionality

BOMD: This popular MD approach allows for simulation of the time evolution of a system of interacting atoms. This is accomplished by integrating Newton's equations of motion for each atom, in which the forces are obtained "on the fly" directly from QM simulations. Despite improvements in HPC, BOMD studies are computationally prohibitive for long simulation times for large systems due to the

large computational cost for the nonlinear self-consistent field (SCF) optimization of the electronic ground state at each integration step.

We explored an enhanced BOMD approach developed to reduce this cost per step, known as the extended Lagrangian-BOMD (XL-BOMD) approach (Niklasson 2008; Niklasson et al. 2009). The idea behind XL-BOMD is that rather than recalculating the density at each step, an extended Lagrangian is used to extrapolate the density, with regular DFT self-consistent calculations periodically performed to update the correct density for further extrapolation. We implemented the original XL-BOMD method into CP2K and found that it provided greater scalability for systems in equilibrium, but worked poorly for material regimes for which bond breaking or bond formation occurred. For example, we found that XL-BOMD simulations of shocked energetic molecular crystals required that the self-consistent cycle be performed at every step in order to get the accuracy needed at the shock front. Thus, this important Army use case could not take advantage of the computational speed-up afforded by the extrapolation of the density in the XL-BOMD approach. Therefore, we no longer pursued the method.

Tight-binding DFT (DFTB). In attempting to improve the applicability of CP2K to treat systems of Army interest larger than full-resolution DFT would allow, we explored semiempirical methods. The DFTB (Elstner et al. 1998) method has proved to be fairly accurate for some systems, somewhat transferable to a broad range of systems and applications, and its computational efficiency lies in between that of DFT and classical reactive atomistic potentials. In addition, DFTB was already implemented in the CP2K program as an order N method. However, the applications of DFTB to Army materials depend on the availability of the atomic input parameters, which were very limited and somewhat system-dependent.

We first assessed DFTB performance in CP2K using as our test system polyethylene (PE). DFTB-MD/CP2K calculations were performed with up to 108,000 atoms and up to 16,384 processors. The performance transition between traditional and O(N) DFTB methods was found to be approximately 8,000 electrons. Parallel efficiency is poor above 4096 processors, with better than linear scaling observed with an increase in the system size (number of atoms). We also evaluated the accuracy of DFTB relative to DFT, by comparing BOMD simulations of the shock Hugoniot of PE; agreement between the QM-DFT was very good from pressures ranging from ambient to 45 GPa (Fig. 2).

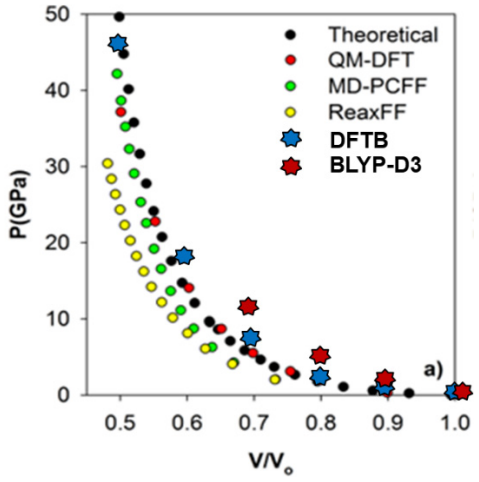

Fig. 2 Pressure vs. relative volume in simulations of compressed PE using different levels of theory (Chantawansri et al. 2012): DFTB and QM-DFT (dispersion corrected atom centered pseudopotential). Becke, 3-parameter, Lee–Yang–Parr (B3LYP)-D3 curves were calculated using CP2K. MD-polymer consistent force-field and reactive bond order-based force field (ReaxFF) curves were calculated using LAMMPS. Theoretical values provided by Carter and Marsh (1995).

A separate calculation assessed DFTB's prediction of optimized crystallographic parameters for the explosive 1,1-diamino-2,2-dinitroethylene (FOX-7); unit cell lengths were within 3%, but overall density was smaller than experiment by 4.75%, outside of the metric of what we consider acceptable performance (3%). Extensive analysis of DFTB performance in predicting properties of RDX was performed; DFTB predictions of crystallographic parameters and density of α-RDX were in acceptable agreement with experiment for pressures up to 10 GPa, as were predictions of shock Hugoniot values. Comparison of DFTB predictions with DFT results are also in reasonable agreement, indicating that DFTB has an overall good performance in predicting RDX properties. However, DFTB failed to predict boron carbide structures, a relevant Army ceramic; since DFTB well predicted carbon structures, we concluded that new DFTB parameters for boron would need to be determined.

We next produced a code that fits the DFTB parameters from reference data; our approach differs from that of others in that we minimized the error in the pressure and forces relative to the reference system under pressure. The difference between the DFT and DFTB energies was captured through the DFTB repulsive term, represented by a polynomial of order N and the cutoff radius. The method was validated in calculations on diamond and PE, with results for cubic diamond shown in Fig. 3.

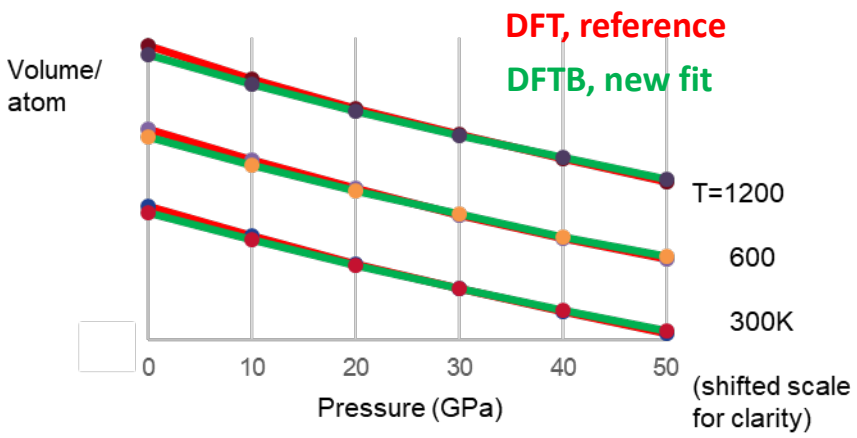

Fig. 3 Comparison of DFTB MD predictions of volume per atom vs. pressure at various temperatures with DFT reference values

Not only do the DFTB values reproduce the DFT (PBE) (Perdew et al. 1996, 1997) values very well, there was no need for adding explicit three-body terms to DFTB within the fitted repulsive term. Transferability of the fitted DFTB potentials was explored in MD simulations of the pressure–volume–temperature properties for diamond allotropes. The DFTB results showed excellent agreement with all DFT reference calculations up to 50 GPa, whereas DFTB results using the original DFTB parameters were in substantially poorer agreement with the DFT reference values for pressures ranging from 0–30 GPa for hexagonal diamond and 0–20 GPa for C8 superhard diamond.

O(N) scaling time-dependent DFT (TD-DFT) methods: TD-DFT allows modeling of optical and electronic properties of materials. This involves determining how the electrons respond to external stimuli within the frequency or time domains. Methods current at the inception of the QMMS program included only the frequency-domain solutions to the time-dependent problem. These frequency-dependent methods have limitations for O(N) methods, because the matrixes are inherently not sparse and the parallelism of these algorithms had not been demonstrated. Time-domain methods allow the use of dynamical simulations in real time (RT), which have been shown to work with O(N) methods. In conjunction with the CP2K development group at the ETH-Zurich, we implemented the RT-TD-DFT method for calculating optical properties. This method is truly an O(N) method for doing time-dependent calculations and has allowed TD-DFT calculations of significantly larger systems than were possible before the implementation of this new method.

QM local stress tensor method. In better understanding the interplay between the mechanical and chemical phenomena occurring in shocked materials (of significant

relevance to the Army), the capacity to calculate local pressure throughout a heterogeneous material is required. Without such a capability, detailed mechanisms of reaction, deformation, or failure of materials subjected to high strain rates cannot be elucidated. Currently, there is no universally accepted QM definition for the local stress tensor, although a classical definition based on atomic contributions is available. In order to provide a QM definition for the local stress tensor, we extended the classical definition to include the electronic contributions. This was accomplished by partitioning the electronic contributions of the global pressure onto atomic centers and adding them to the atomic contributions within the QM definition. We implemented the approach into CP2K and validated it against well-known properties of the local pressure for diamond (i.e., the average of local pressure equals the global pressure, the atomic pressure is uniform in a homogeneous system).

A more difficult validation of the approach was found in a BOMD simulation of overdriven shock in the high explosive pentaerythritol tetranitrate (PETN). This system is an example of Army-relevant materials subjected to high strain rates. The simulation cell was of 32 × 2 × 2 unit cells of PETN, thus comprising 256 PETN molecules (7,424 atoms). This simulation cell was equilibrated at 300 K using isothermal-isochoric (NVT) MD and a timestep of 0.25 fs. For the shock simulation, the eight rightmost molecules shown in Fig. 4 were kept rigid, while the 64 leftmost molecules are used as a flyer plate. For all simulations, periodic boundary conditions were imposed in the directions perpendicular to shock propagation.

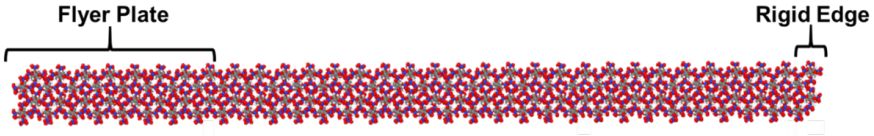

Fig. 4 Schematic of the PETN filament at the beginning of the simulation

At the initiation of the shock simulation, the atomic velocity of each flyer plate atom was increased by 10 km/s in the shock direction (i.e., from left to right in Fig. 4). The subsequent microcanonical (NVE) MD simulation was performed for 1.563 ps (with an elapsed RT of greater than 18 months utilizing the US Army Engineer Research and Development Center, Navy, and DEVCOM ARL DOD Supercomputing Resource Center). The simulation was terminated as the shock front was reaching the rigid far-right edge of the filament; to continue the simulation, more material would need to be added. The local pressure calculation was not performed "on the fly," but instead used in postprocessing, providing the following result shown in Fig. 5 for a snapshot at 1.25 ps.

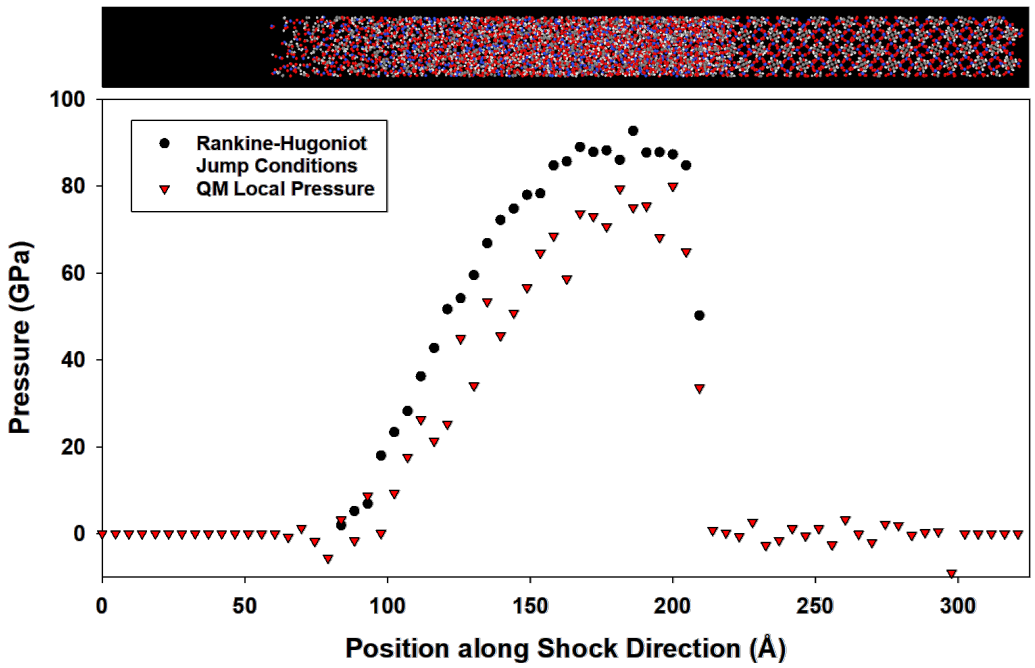

Fig. 5 (Upper) Snapshot of atomic positions at 1.25 ps in BOMD simulation of shocked PETN. (Lower) Local pressure as a function of position along the shock direction.

In Fig. 5, each point represents the averaged value within a volume having dimensions of 1/2 × 2 × 2 unit cells of PETN at 300 K, 1 atm. We have also provided the estimated pressure as given by the Rankine–Hugoniot jump conditions based on the particle (u_P) and shock velocities (U_S) measured by us in this simulation (i.e., $P = \rho_0 U_S u_P$, where ρ_0 is the mass density of PETN in the ambient state). The agreement between those estimates and the QM predictions is very good.

Fast, accurate MD using delta-ML potentials. The computational costs of the BOMD simulation of overdriven shock in PETN described previously highlights a need for enabling a capability that will provide high-fidelity precision in MD simulations with computational costs at or near that of low-fidelity models. One such possibility is to create and enable delta-ML approaches to predict differences between quick, low-accuracy and slow, higher-accuracy models used in atomistic simulations. These ML corrections are then used to increase the accuracy of the predictions of the low level model.

Toward that end, we have implemented a Gaussian Process Regression (GPR) machine-learned delta model (MLDM) in LAMMPS. The MLDM captures the difference between an expensive, high-fidelity model and a fast, low-fidelity MD model as specified by the user. The low-fidelity model can then be used with the MLDM, under the conditions that it has been trained for, to give high-fidelity results at a computational cost similar to the low-fidelity model. An MLDM can be

constructed to connect any two models accessible in LAMMPS. To date, the capabilities have been tested for classical potentials; however, any QM models can be used by linking the QM suite with LAMMPS; this has been done for DFTB (using the LLNL code Latte) and DFTB+ (Hourahine et al. 2020) (using an LLNL-developed callback function). At this time, we are pursuing linking CP2K with LAMMPS in a similar fashion. Also, we are working with the High Performance Computing Modernization Program's (HPCMP's) User Productivity Enhancement and Training (PET) program to implement an automated just in time (JIT) or speculative model update into the MLDM. As potentials based on GPR natively calculate their uncertainty, model confidence can be assessed during a dynamics simulation. When the estimates exceed a user-specified precision threshold, a high-fidelity simulation can be performed, with its result used to update the MLDM during the simulation. In this way, the model will be updated only as needed.

Electron transport: In support of EMRM efforts to develop modeling capabilities for semiconductor materials and devices, we undertook to enable a capability to calculate accurate electron transport for systems with interfaces and defects. As a result, a program package called Transire was developed and provided as open-source software (Carlin and Rinderspacher n.d., 2017). This software package enables the efficient exploration and optimization of grain boundary domains, including rotations, translations, and Miller indices, as well as compute (electron) transport properties across the grain boundary. For full documentation of capabilities, see Carlin and Rinderspacher (2017). It integrates with the highly scalable HPC packages CP2K and LAMMPS to access the necessary large interface regions.

Transire has been successfully used to predict gallium nitride (GaN)/silicon carbide interfaces and electron transport through bridging molecules (Carlin and Rinderspacher 2017, 2019). It has further been used to optimize cleavage surfaces by coupling it to machine-learned surrogates.

3.2 Multi-Resolution DFT

QC-DFT: We collaborated with the group of Professor Vikram Gavini at the University of Michigan on development of real-space methodologies for large-scale DFT simulations. These methodologies employ a conventional FE basis to solve both the orbital free and KS-DFT equations (Gavini et al. 2007; Motamarri et al. 2013; Lee et al. 2015) The FE basis offers numerous advantages over traditional approaches, such as the plane-wave basis, as it allows for coarse-graining, has excellent scalability on parallel computing platforms, and can handle complex geometries and boundary conditions. The use of a high-order FE basis with

specialized spectral Gauss–Lobatto quadrature leads to an efficient numerical algorithm for solving the discrete eigenvalue problem in KS-DFT.

Comparison of the developed FE method to ABINIT (Gonze et al. 2020), a widely used DFT software that uses the plane-wave basis, was performed for electronic structure calculations of large clusters of aluminum atoms. The computational cost of the FE basis was found to be less than ABINIT with comparable error in ground state energy. For an aluminum cluster of 1688 atoms, ABINIT is not able to compute a solution due to its large memory requirements, whereas the FE method successfully obtains the electronic structure. More recently, Professor Gavini's group has extended the method to include an enriched FE basis (Kanungo and Gavini 2017), applied the method to TD-DFT (Kanungo and Gavini 2019), and formulated algorithms to compute configurational forces for geometry optimization (Motamarri and Gavini 2018). Professor Gavini's group released the open-source software DFT-FE and demonstrated its capability to perform electronic structure calculations of systems containing 50,000 to 100,000 electrons with scalability demonstrated up to 192,000 processors (Motamarri et al. 2020).

EE-DFT: Our approach was to expand upon a concept introduced to overcome limitations in orbital-free embedded-density functional theory (E-DFT) (Cortona 1991; Wesolowski and Warshel 1993; Govind et al. 1998; Wesołowski 2006), which provides a framework for dividing a system's total electron density into subsystems to be calculated separately. The E-DFT hypothesis is that subsystems composing a larger system, each defined by its electron density, interact solely via their electronic densities. If true, the subsystems could be used in the QM equations. Furthermore, the approach is massively parallelizable. The E-DFT approach allows for potential computational cost savings, as the subsystems can be treated with varying degrees of QM accuracy, including subsystems that are adequately treated using extremely low levels of theory. Unfortunately, its original formulation was to applications involving nonbonded or weakly interacting molecular groups, and shown to fail for covalently bonded embedded subsystems.

The EE-DFT provided a "general and formally exact protocol for treating the nonadditive kinetic potential" in E-DFT, the source of significant error (Goodpaster et al. 2010), and was shown to successfully describing breaking of covalent bonds and hydrogen bonds with chemical accuracy (Goodpaster et al. 2011). Conceptually, the EE-DFT formalism allows for the partitioning of heterogeneous macroscale systems into material subsystems ranging from the atomistic up through the continuum. Following that concept, we were interested in applying the methodology to the full multiscale system, partitioning it into subsystems of different scales (i.e., atomistic, meso, and continuum subsystems). The electron density for each subsystem would be determined independently (and in parallel),

with the results from the subsystem calculations stitched together using the QM equations without introducing error. Before attempting this modification, we applied the EE-DFT methodology to a variety of partitions, with the first being the most simple, in which the systems could be partitioned neatly into individual molecules. For this simple case, we tested partitioning water into different subsystems:

- Trimer system: Three individual molecules
- Pentamer system: Five individual molecules, two subsystems, three subsystems, and permutations on these
- Decamer: Ten individual molecules

Errors were very reasonable, ranging from less than 0.2 kcal/mol up to 1.4 kcal/mol (for the decamer). The next set of calculations involved complex polymer partitions to test three major questions: 1) effect of bond cleavages across partitioning, 2) effect of separation distance of partitioned systems, and 3) effect of size of partitioned systems. The calculations did not proceed as smoothly as systems with natural partitioning into individual molecules, with the discovery that partitioning must result in "closed" subsystems (i.e., no radical moieties). In general, large errors were seen due to convergence issues regardless of prototype polymer system.

To test the most complex types of molecules, those with delocalization and multiple bonds, we studied benzene and the explosive triamino trinitrobenzene (TATB). Benzene was completely non-convergent, with egregiously large oscillations in the "converging" energy, with similar errors seen for TATB. Finally, as a simple prototype of armor materials, we studied the B_{12} cluster, a unit of the B_{12}-CCC structure in boron carbide. No conclusive results were achieved due to non-convergence issues. Not only did it fail to produce accurate results, it required a computationally demanding matrix inversion that would limit application to small systems. While we understand that later iterations of this method replaced the rigorously correct matrix inversion with a less computationally demanding approximation, we did not further pursue this interesting idea.

QM/molecular modeling (MM): QM/MM is a currently well-developed embedding methodology use to model the atomic scale. While the general technique is more mature than the other efforts in this program, the maturity for a given procedure for any specific material system can wildly vary. For example, no reliable force fields for accurate prediction of polarization are available for hybrid QM/MM calculations for battery materials. As polarization can have a strong effect on a wide range of materials (Bedrov et al. 2019), we address this deficiency within this task. Two approaches were pursued. One is the development and applications of the

many-body polarizable force fields based on the point permanent charges and screened atomic dipoles to a wide range of ionic materials from liquid electrolytes to ionic liquids, polymer electrolytes, and crystalline solid electrolyte interphase (SEI) components. The second approach is to further improve predictive capabilities by modifying the functional form of the Atomistic Polarizable Potential for Liquids, Electrolytes, and Polymers (APPLE&P) force field by including Gaussian electrostatics and implementing it in the community-supported MD simulation code Tinker-HP. MD simulation of bulk and electrochemical interfaces are combined with DFT calculations to provide mechanisms for reductive and oxidative decomposition of electrolyte components (Borodin et al. 2017a; Borodin 2019).

MD simulations using developed force field parameters for the APPLE&P force field accurately predicted electrolyte structure and transport, and established a connection between the cation first solvation shell and preferential reduction obtained from DFT calculations and experiments, and complemented DFT studies of the reactivity and bare and passivated electrode materials (Allen et al. 2014; Bauschlicher et al. 2014; Borodin 2014, 2019; Borodin and Bedrov 2014; Geiculescu et al. 2014; Han et al. 2014, 2015; Haskins et al. 2014; Hu et al. 2014; Jow et al. 2014; Lesch et al. 2014, 2016; McOwen et al. 2014; Seo et al. 2014; Smith et al. 2014; Wang et al. 2014, 2018a, 2018b, 2019; Barnes et al. 2015; Borodin et al. 2015a, 2015b, 2015c, 2016a, 2106b, 2017a, 2017b, 2018, 2020; Islam et al. 2015; Kim et al. 2015a, 2015b; Knap et al. 2015; Li et al. 2015, 2019; Qian et al. 2015; Suo et al. 2015, 2016, 2017a, 2017b; von Wald Cresce et al. 2015; Wu et al. 2015, 2017a, 2017b, 2018, 2020; Delp et al. 2016; Deng et al. 2016; Gu et al. 2016; He et al. 2016; Luo et al. 2016, 2018; McClure et al. 2016; Mogurampelly et al. 2016; Vatamanu et al. 2016, 2017a, 2917b, 2018; Wan et al. 2016; Bedrov et al. 2017, 2019; Chapman et al. 2017; Cresce et al. 2017; Lu et al. 2017; Price et al. 2017; Vatamanu and Borodin 2017; Yang et al. 2017a, 2017b, 2019a, 2019b, 2020; Alvarado et al. 2018, 2019; Bieker et al. 2018; Fan et al. 2018; Peng et al. 2018; Song et al. 2018, 2020; Steinrück et al. 2018, 2020a, 2020b; Zhang et al. 2018, 2020, 2021; Zhao et al. 2018; Huang et al. 2019; Mao et al. 2019; Raberg et al. 2019; Chen et al. 2020a, 2020b, 2020c, 2020d; Cho et al. 2020b; González et al. 2020; Henderson et al. 2020; Jiang et al. 2020; Ma et al. 2020a, 2020b, 2021a, 2021b; von Aspern et al. 2020; Zhou et al. 2020; Cao et al. 2021a, 2021b; Davies et al. 2021; Glaser et al. 2021; Ho et al. 2021; Hou et al. 2021a, 2021b, 2021c; Shadike et al. 2021; Widstrom et al. 2021).

Specifically, MD simulations of the electrified electrode–electrolyte interfaces provided molecular scale insight into the behavior of carbonate-based lithium (Li)-salt-based electrolyte at graphite electrodes (Vatamanu et al. 2012) and uncovered

a mechanism for extending water-in-salt electrolyte (WiSE) oxidation stability and cathodic challenges for stabilizing WiSE and hybrid electrolytes (Borodin et al. 2017a; Vatamanu and Borodin 2017; Yang et al. 2017a; Chen et al. 2020c). Electrical double layer (EDL) structure of the hybrid zinc (Zn) electrolyte combined with a detailed DFT analysis suggested a mechanism for forming a robust SEI for aqueous Zn electrolyte that resulted in an aqueous Zn battery in which a dilute and acidic aqueous electrolyte with an alkylammonium salt additive assists the formation of a robust, Zn^{2+}-conducting and waterproof SEI (Cao et al. 2021b). The presence of this SEI enables excellent performance: dendrite-free Zn plating/stripping at 99.9% coulombic efficiency in a titanium (Ti)||Zn asymmetric cell for 1,000 cycles; steady charge–discharge in a Zn||Zn symmetric cell for 6,000 cycles (6,000 h) (Cao et al. 2021b). A combination of MD of bulk electrolytes, EDL simulations, and DFT studies of the reduction and oxidation reactions also guided development of alkyl phosphonium-additives to aqueous Zn electrolytes (Ma et al. 2021b).

A combination of DFT calculations, MD simulations led to discovery of WiSEs for Li batteries in collaboration with University of Maryland group's (Suo et al. 2015; Yang et al. 2017a) (2016 University of Maryland Invention of the Year Award), development of the high-energy-density halide intercalation graphite cathode (Yang et al. 2019a) and extension of this approach to Zn batteries (Wang et al. 2018b).

Rechargeable Mg and calcium metal batteries (rechargeable magnesium batteries [RMBs] and rechargeable calcium batteries [RCBs]) are promising alternatives to Li-ion batteries because of the high crustal abundance and capacity of Mg and calcium. Yet, they are plagued by sluggish kinetics and parasitic reactions. A combination of MD simulations and DFT calculations of the outer sphere electron transfer kinetics and interfacial electrochemistry guided a search for chelants that greatly promote interfacial charge transfer kinetics and suppress side reactions on both the cathode and metal anode through solvation sheath reorganization, thus enabling stable and highly reversible cycling of the RMB and RCB full cells with energy densities of 412 and 471 W·h/kg, respectively. This work provided a versatile electrolyte design strategy for divalent metal batteries (Hou et al. 2021a).

ReaxFF (Islam et al. 2015) and non-reactive MD simulations (Wu et al. 2020; Glaser et al. 2021; Yang et al. 2017b) and DFT calculations (Wu et al. 2018; Luo et al. 2016; Bieker et al. 2018; Zhang et al. 2020) of Li-sulfur (S)–based electrolytes guided improvement Li-S battery performance to enable better electrode wetting, greatly improved high-rate capability, stable cycle performance for high S loading cathodes and low electrolyte/S ratio in Li-S cells, and the extraordinary ability of

such electrolyte systems to suppress short-chain polysulfide dissolution and polysulfide shuttle effects.

The newly developed projection-based embedding method was jointly applied to understanding electrolyte oxidation. It corrected qualitative inaccuracies in the electronic densities and ionization energies obtained from conventional KS-DFT methods. Our wave function-in-DFT embedding approach enables accurate calculation of the vertical ionization energy (IE) of individual molecules at the CCSD(T) level of theory while explicitly accounting for the solvent using a combination of DFT and molecular mechanics interactions, as shown in Fig. 6 (Barnes et al. 2015).

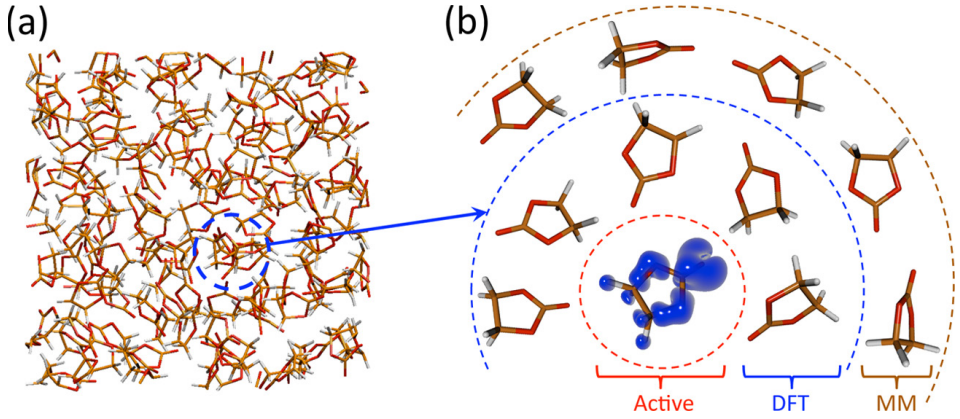

Fig. 6 Summary of the embedding protocol. (a) MD simulations are performed to generate the equilibrium ensemble of solvent configurations. (b) An embedded CCSD(T) calculation is performed on a single molecule from the MD simulation (the "active region"), indicated by the red circle. The electron hole created upon oxidation of the active region is illustrated by the blue electron cloud. Nearby molecules are treated at the B3LYP level, indicated by the blue circle. More distant molecules are treated using a point-charge MM model, indicated by the brown circle.

We found that the ensemble-averaged distributions of vertical IEs are consistent with a linear response interpretation of the statistics of the solvent configurations, enabling determination of both the intrinsic oxidation potential of the solvents and the corresponding solvent reorganization energies (Barnes et al. 2015). Interestingly, we reveal that large contributions to the solvation properties of dimethyl carbonate (DMC) originate from quadrupolar interactions, resulting in a much larger solvent reorganization energy than that predicted using simple dielectric continuum models. Demonstration that the solvation properties for two molecules of interest to Li battery electrolytes, ethylene carbonate (EC) and DMC, are governed by fundamentally different intermolecular interactions provides insight into key aspects of Li-ion batteries, with relevance to electrolyte decomposition processes, SEI formation, and the local solvation environment of Li cations.

4. Mesoscale Modeling of Dislocation Evolution in the Presence of Microstructure

The mechanical and electronic properties of crystalline materials are strongly influenced by the presence and evolution of dislocations. The evolution of dislocations is, in turn, greatly affected by a wide variety of microstructural features commonly present in crystalline materials, such as surfaces, interfaces, grain boundaries, and precipitates. The goal of this project was to develop computational methodologies (i.e., numerical methods and associated algorithms) to enable accurate predictions of dislocation evolution in crystalline materials with microstructure. Through predictive modeling of dislocation–microstructure interactions, novel microstructures can be designed and tested on a computer. For example, the size, shape, and distribution of nanoscale precipitates could be optimized to impede dislocation motion for increased yield strength and hardening behavior of Mg alloys for lighter vehicle armor. Or free surface and interface geometry could be optimized to facilitate dislocation annihilation in GaN thin films to improve efficiency in high-powered electronics. The process of exploring these design spaces takes years, if not decades, with the traditional "build and test" paradigm. Computational design can drastically accelerate the pace of innovation in improving material properties.

At the onset of this project, it was computationally intractable to accurately model dislocation evolution in crystalline materials with microstructure. A discrete treatment of dislocations and microstructural features is necessary for accurate models of dislocation multiplication, pileup, and annihilation. Yet, discrete treatments of these features cause an exponential growth in the number of degrees of freedom due to the large number of interacting dislocations and microstructural features that are present in crystalline materials. Furthermore, high gradients in the stress fields surrounding both dislocations and microstructure require fine resolution at the spatial and temporal scales. While larger and larger HPC resources would be able to address these computational challenges, a fundamental obstacle to efficient, large-scale simulations was the inherent incompatibility in domain decomposition and load balancing between the numerical treatments of dislocations and microstructure.

The SOA in the explicit modeling of dislocations is the discrete dislocation dynamics (DDD) method, while the FE method is the most effective and efficient method for computing the stress fields of arbitrarily shape microstructural features. Due to the rapid multiplication of dislocations during a DDD simulation, dynamic load balancing is desired, where the boundaries of the parallel domain decomposition evolve to maintain an equal number of dislocation segments on each

process. In contrast, the FE computations are most efficient with a static domain decomposition strategy, where the number of elements on each processor are equal. Additionally, the relative computational cost of the FE and DDD calculations will vary if, for example, one is modeling a few dislocation segments in a highly refined FE mesh versus modeling hundreds of thousands of dislocation segments in a coarse FE mesh. Due to these computational challenges, simulation capabilities for incorporating microstructure into DDD simulations were limited to serial academic codes that could only model a few dislocations interacting with a single microstructural feature. Scalable algorithms and codes capable of modeling realistic densities of dislocations and microstructure were nonexistent.

Three components were required to achieve the required scalability and efficiency for modeling realistic dislocation–microstructure interactions. First, a method for computing interaction forces between dislocations that is highly scalable and efficient on HPC resources is needed. For this component, the project leveraged the Parallel Dislocation Simulator (ParaDiS) (Arsenlis et al. 2007) developed at LLNL. ParaDiS has proven to be the SOA for single-crystal DDD simulations on HPC architectures. Therefore, it made a logical foundation on which the algorithms for incorporating microstructural effects could be added. The ParaDiS development team at LLNL was frequently consulted throughout this project to ensure the microstructure effects were incorporated accurately and efficiently and to leverage their expertise in DDD simulations. The second component was a FE-based method for computing the forces on dislocations due to the presence of microstructure. This capability did not exist in any simulation tools and would therefore need to be developed. The third and final component was a method for load balancing the DDD and FE calculations, while maintaining separate domain decomposition strategies to ensure parallel scalability. To achieve the desired flexibility, the FE calculations were developed into a separate executable, rather than integrating the FE calculations directly into existing DDD software, following the multiple-program-multiple-data (MPMD) paradigm. This allows a user to independently select the number of CPU resources for the FE and DDD components and enables the use of independent domain decomposition strategies. A tightly coupled communication pattern was established between the DDD and FE codes to enforce concurrency during the phases of the simulation with the highest computational expense. A parallel virtual filesystem was employed to efficiently share data between simulators. Coupling of FE to the DDD simulators was achieved through the use of an HDF5-based distributed shared memory (DSM) library (Soumagne et al. 2010).

In addition to the algorithmic developments, additional physical insights were needed before microstructural effects could be accurately modeled in the

representative crystalline materials, Mg and GaN. Both these materials follow the hexagonal close-packed (HCP) crystal structure. Modeling of dislocations in HCP structures was limited in comparison face-centered cubic (FCC) and body-centered cubic (BCC) crystals. Therefore, theoretical, numerical, and experimental techniques were employed to further elucidate the structure and mobility of dislocations in HCP materials, so that the FE-DDD simulations could incorporate the unique behavior of dislocation evolution in HCP materials.

Initial studies were focused on assessing and improving the computational efficiency and parallel scalability of the coupled FE-DDD simulator. In Leiter et al. (2013), a strong scalability study was performed where the size of the simulation was fixed as the number of CPUs was varied. The results showed good parallel efficiency on over 1,000 CPUs. The study also varied the ratio of processors dedicated to the FE and DDD executables, demonstrating effective load balancing between applications. Finally, profiling of each phase in the FE computation was performed and revealed that the primary computational expense was in the linear solve of the elastostatic boundary value problem.

Based on the profiling results, an emphasis was placed on improving the linear solvers and preconditioners employed in the FE calculations. New iterative and direct solvers were incorporated in the FE code to speed up the linear solve. A comprehensive study on the efficiency and scalability of these solvers under a variety of preconditioners was performed in Crone and Munday (2014). It was found that the new iterative solver, based on the HYPRE (Falgout and Yang 2002) library, provided a 10× speedup on the solve time over the existing iterative solver by employing an algebraic multigrid (AMG) preconditioner. Through a high-dimensional parametric study of the AMG parameters, a combination of parameters was found that produced the best serial and parallel efficiency across a range of FE mesh sizes. The direct solver, based on the Multifrontal Massively Parallel Solver (MUMPS) (Amestoy et al. 2001) library, provided a 100× speedup on the solve time over the existing iterative solver. However, the initial setup time and memory usage grew rapidly with increasing FE mesh size; therefore, the direct solver was found to be best suited for small- to medium-sized FE meshes.

Following successful demonstrations of the efficiency and scalability of the FE-DDD simulator, a large-scale simulation was performed in Crone et al. (2014). The large-scale simulation in this work showed the strong attraction between dislocations and free surfaces, creating a gradient in the density of dislocations throughout the thickness of a film. The simulation was the largest DDD simulation with microstructure at the time, in terms of the number of dislocation segments and the size of the FE model mesh used to represent the microstructure. The simulation

highlighted the unique capability of the FE-DDD simulator developed in this project.

In conjunction with the algorithmic developments for the FE-DDD simulator, various theoretical and numerical studies were conducted to gain a better understanding of dislocation evolution in HCP crystals (Wu et al. 2012, 2013, 2014, 2016). These studies characterized the strength of junctions formed when two or more dislocations connect. This junction strength is critical in determining the strain hardening effect and the stress required to induce dislocation motion to promote annihilation. Theoretical and experimental characterization of dislocations in GaN provided new insight in the formation and core structures (Batyrev et al. 2011, 2013, 2017; Jones and Batyrev 2012; Krimsky et al. 2018). The Peierls stress and glide mobility of dislocations in GaN were quantified through atomistic simulations (Weingarten and Chung 2013; Weingarten 2015, 2018; Weingarten and Larentzos 2015) and experiments (Krimsky et al. 2018). These quantities determine the amount of stress required for a dislocation to start moving in a crystal and the speed at which it moves under an applied stress. Through these studies, it was discovered that the barriers for dislocation motion in GaN were significantly higher than hypothesized. Due to this discovery, the focus for eliminating dislocation in GaN thin films shifted from how to remove dislocations, to preventing them from forming in the first place. While this new direction was outside of the scope of the modeling capabilities being developed with the FE-DDD simulator, it was an important result that shifted focus to developing novel methods for GaN thin-film growth, such as ammonothermal growth (Liu et al. 2020).

Due to the difficulty in inducing dislocation motion in GaN, the modeling focus of the FE-DDD simulator was shifted from semiconductors to structural metals. In particular, studying the effects of voids and nanoscale precipitates, which were found to be an effective microstructure for improving spall strength in Mg alloys (Mallick et al. 2021). The nucleation of prismatic dislocation loops (PDLs) from nanoscale voids and precipitates was studied in a series of FE-DDD simulations (Munday et al. 2015, 2016). The formation of PDLs induces void growth and precipitates decoherence, which are important phenomena in high-rate loading conditions. The studies found a strong pressure dependence on PDL formation, as well as variability in the PDL mechanisms among FCC, BCC, and HCP crystals. The strengthening effect of voids and precipitates is due to their collective ability to impede dislocation motion, which delays the onset of plastic deformation to higher stresses and strains.

Quantifying the strengthening effects of obstacle arrays was the focus in a series of papers (Crone et al. 2015; Szajewski et al. 2019, 2020, 2021). These papers used a combination of theory and numerical simulations to determine the effects of

obstacle size, shape, and distribution on yield strength. Due to the modeling capabilities of the FE-DDD simulator, the effect of obstacle type (i.e., void vs. soft inclusion vs. hard inclusion) was also quantified, resulting in an analytical model that can predict the strengthening effect of obstacles without the need for additional simulations.

The FEM-DD simulator also demonstrated the ability to capture stochasticity in small-scale plasticity (Crone et al. 2018; Szajewski et al. 2022). Stochasticity becomes important in micro- and nanotechnology, where the presence of a few defects can drastically change the material strength. FEM-DD is well suited to explore these effects because dislocations are explicitly modeled and free-surface effects are captured, which dominate at these scales due to the high surface-to-volume ratios.

Recently, the collection of algorithms developed through this project were implemented in a robust software package called Finite Elements for Discrete Dislocation Dynamics (FED3) (Crone et al. 2021). This software has been incorporated into the development branch of ParaDiS, allowing other researchers throughout DOD and Department of Energy to use and expand this modeling capability. Through a collaboration between DEVCOM ARL, LLNL, and NASA, the modeling capabilities of FED3 are currently being extended to include dislocation transmission between grain boundaries (Cho et al. 2020a).

The algorithms developed in the project resulted in a modeling capability that was 2 orders of magnitude faster than the previous SOA by focusing on algorithms that efficiently scale on HPC resources. The capabilities enabled the modeling of dislocation–microstructure interaction at a fidelity that was previously unattainable. However, the cost of FE-DDD simulations is still too high to serve as a replacement for analytical and empirical constitutive models in macroscale simulations. Therefore, the FE-DDD method is best suited as part of a multiscale approach to modeling plasticity by capturing mesoscale phenomena. Information gleaned from these simulations can inform constitutive models, replacing many of the time-consuming experiments required to develop constitutive models for novel materials.

Impacts of this project reach beyond the study of dislocations by proving the viability of a DSM approach to coupling multiphysics and multiscale applications. The DSM communicator enabled the coupling of two disparate codes that relied on drastically different numerical algorithms and parallelization strategies. The coupling also required large amounts of data to be transferred between codes numerous times over the course of a simulation. Despite these challenges, the coupled application was found to scale efficiently on HPC resources.

However, the DSM-based approach is labor intensive, as significant modifications are required to each code in the coupled applications. Furthermore, a strict communication pattern must be enforced. If large amounts of data must be communicated between applications and if the time and resources are available to implement a DSM coupling, then the approach can provide excellent performance. In contrast, the HMS coupling approach, also discussed in this report, provides a generic coupling framework that requires minimum time and resources to couple multiphysics and multiscale models. The HMS approach requires little, if any, modifications to existing software and is better suited for asynchronous and unpredictable communication patterns. However, the added flexibility comes at the cost of additional overhead in the communication and execution. These insights into the benefits and tradeoffs for various coupling strategies are critical to determining the appropriate approach in future multiphysics and multiscale coupling applications.

4. Conclusions and Path Forward

In summary, the cross-cutting effort was aimed squarely at developing new methodologies to improve predictive capabilities of multiscale modeling when applied to materials. The effort evolved around three thrusts crucially important in multiscale modeling of materials. In all, the research performed under the auspices of the cross-cutting effort yielded a number of important scientific results relevant not only to DEVCOM ARL researchers but also to the scientific community at large. For example, the scale-bridging project facilitated construction of a new multiscale model of the explosive RDX capable of capturing complex mechano-chemistry under STEX conditions. Software improvements to SOA large-scale QM codes allowed for the first-ever full-resolution DFT simulation of overdriven shock in a solid PETN filament composed of 7,424 atoms for approximately 1.6 ps, the largest simulation of its type to date. Further, augmentation to capabilities provided a first-ever first-principles description of local pressure of the material behind the propagating shock front. Multi-resolution capabilities included advancements in hybrid QM/MM calculations for battery materials, which provided insight into key aspects of Li-ion batteries and provided an electrolyte design strategy for alternative divalent metal batteries. Finally, the work on the effects of voids and precipitates on small-scale plasticity enabled discovery of an effective microstructure for improving spall strength in Mg alloys.

The legacy of the cross-cutting effort goes beyond just scientific results. The HMS scale-bridging software library remains under active development and continues to be employed to construct multiscale material models for Army applications. Efforts are underway to release the source code of the HMS library to ensure that the library

can be utilized for multiscale modeling by DEVCOM ARL's collaborators. In this context, the HMS-VUMAT appears particularly advantageous as it markedly reduces the cost of building a multiscale material model. Moreover, the improvements in linear scaling and RT-TD-DFT methods have been transitioned to the CP2K suite, with work continuing to link LAMMPS with CP2K. The link will enable use of DFT models within LAMMPS, including with the MLDM we implemented for use with a fast, low-fidelity MD model in LAMMPS to produce high-accuracy results. Finally, with the sunset of the cross-cutting effort, the FED3 software has been transitioned to LLNL and will continue to have a lasting impact on small-scale plasticity modeling for years to come.

It is also important to emphasize the legacy of the cross-cutting effort in terms of scientific project management. In contrast to projects at DEVCOM ARL aimed at development of specific technologies, the cross-cutting effort was primarily a method development program. Hence, its main objective was not geared toward addressing a particular scientific or engineering problem, but instead on developing methods to facilitate seeking solutions of a broad classes of problems by computational means. To that end, the effort required multidisciplinary teams, and all three projects involved researchers from the Computational and Information Sciences Directorate, the Sensors and Electron Devices Directorate, and the Weapons and Materials Research Directorate at DEVCOM ARL. This multidisciplinary aspect cannot be overemphasized as it fostered deep and lasting collaborations across all the directorates involved. The cross-cutting effort appears an excellent model for removing organizational barriers and fostering meaningful collaborative research endeavors.

5. References

Allen JL, Borodin O, Seo DM, Henderson WA. Combined quantum chemical/Raman spectroscopic analyses of Li+ cation solvation: cyclic carbonate solvents—ethylene carbonate and propylene carbonate. J Power Sources. 2014;267:821–830.

Alvarado J, Schroeder MA, Pollard TP, Wang X, Lee JZ, Zhang M, Wynn T, Ding M, Borodin O, Meng YS, et al. Bisalt ether electrolytes: a pathway towards lithium metal batteries with Ni-rich cathodes. Ener Env Sci. 2019;12:780–794.

Alvarado J, Schroeder MA, Zhang M, Borodin O, Gobrogge E, Olguin M, Ding MS, Gobet M, Greenbaum S, Meng YS, et al. A carbonate-free, sulfone-based electrolyte for high-voltage Li-ion batteries. Materials Today. 2018;21:341–353.

Amestoy PR, Duff IS, L'excellent JY, Koster J. MUMPS: A general purpose distributed memory sparse solver. Applied Parallel Computing, Proceedings. 2001;1947;121–130.

Arsenlis A, Cai W, Tang M, Rhee M, Oppelstrup T, Hommes G, Pierce TG, Bulatov VV. Enabling strain hardening simulations with dislocation dynamics. Modelling and Simulation in Materials Science and Engineering. 2007;15:553–595.

Barnes BC, Leiter KW, Becker R, Knap J, Brennan JK. LAMMPS integrated materials engine (LIME) for efficient automation of particle-based simulations: application to equation of state generation. Modelling and Simulation in Materials Science and Engineering. 2017;25.

Barnes BC, Leiter KW, Larentzos JP, Brennan JK. Forging of hierarchical multiscale capabilities for simulation of energetic materials. Propellants Explosives Pyrotechnics. 2020;45:177–195.

Barnes TA, Kaminski JW, Borodin O, Miller TF. Ab initio characterization of the electrochemical stability and solvation properties of condensed-phase ethylene carbonate and dimethyl carbonate mixtures. J Phys Chem C. 2015;119:3865–3880.

Batyrev IG, Sarney WL, Zheleva TS, Nguyen C, Rice BM, Jones KA. Dislocations and stacking faults in hexagonal GaN. Physica Status Solidi a-Applications and Materials Science. 2011;208:1566–1568.

Batyrev IG, Weingarten NS, Jones KA. Simulations of dislocation core in pyramidal plane of n- and p-doped wurtzite GaN and AlGaN. Physica Status Solidi B-Basic Solid State Physics. 2017;254.

Batyrev IG, Wu C, Chung PW, Weingarten NS, Jones KA. Control of defects in aluminum gallium nitride ((Al) GaN) films on grown aluminum nitride (AlN) substrates. Army Research Laboratory (US); 2013. Report No.: ARL-TR-6350.

Bauschlicher CW, Haskins JB, Bucholz EW, Lawson JW, Borodin O. Structure and energetics of Li^{+}-$(BF_4^-)_n$, Li^{+}-$(FSI^-)_n$, and Li^{+}-$(TFSI^-)_n$: ab initio and polarizable force field approaches. J Phys Chem B. 2014;118:10785–10794.

Bedrov D, Borodin O, Hooper JB. Li^+ transport and mechanical properties of model solid electrolyte interphases (SEI): insight from atomistic molecular dynamics simulations. J Phys Chem C. 2017;121:16098–16109.

Bedrov D, Piquemal J-P, Borodin O, Mackerell AD, Roux B, Schröder C. Molecular dynamics simulations of ionic liquids and electrolytes using polarizable force fields. Chemical Reviews. 2019;119:7940–7995.

Bieker G, Diddens D, Kolek M, Borodin O, Winter M, Bieker P, Jalkanen K. Cation-dependent electrochemistry of polysulfides in lithium and magnesium electrolyte solutions. J Phys Chem C. 2018;122:21770–21783.

Borodin O. Molecular Modeling of Electrolytes. In: Jow TR, Xu K, Borodin O, Ue M, editors. Electrolytes for lithium and lithium-ion batteries. Springer; 2014.

Borodin O. Challenges with prediction of battery electrolyte electrochemical stability window and guiding the electrode – electrolyte stabilization. Current Opinion in Electrochemistry. 2019;13:86–93.

Borodin O, Bedrov D. Interfacial structure and dynamics of the lithium alkyl dicarbonate SEI components in contact with the lithium battery electrolyte. J Phys Chem C. 2014;118:18362–18371.

Borodin O, Giffin GA, Moretti A, Haskins JB, Lawson JW, Henderson WA, Passerini S. Insights into the structure and transport of the lithium, sodium, magnesium, and zinc bis(trifluoromethansulfonyl)imide salts in ionic liquids. J Phys Chem C. 2018;122:20108–20121.

Borodin O, Han S-D, Daubert JS, Seo DM, Yun S-H, Henderson WA. Electrolyte solvation and ionic association: VI. acetonitrile-lithium salt mixtures: highly associated salts revisited. J Electrochem Soc. 2015a;162:A501–A510.

Borodin O, Olguin M, Ganesh P, Kent PRC, Allen JL, Henderson WA. Competitive lithium solvation of linear and cyclic carbonates from quantum chemistry. Phys Chem Chem Phys. 2016a;18:164–175.

Borodin O, Olguin M, Spear C, Leiter K, Knap J, Yushin G, Childs A, Xu K. Challenges with quantum chemistry-based screening of electrochemical stability of lithium battery electrolytes. ECS Transactions. 2015b;69:113–123.

Borodin O, Olguin M, Spear CE, Leiter K, Knap J. Towards high throughput screening of electrochemical stability of battery electrolytes. Nanotechnology. 2015c;26:354003.

Borodin O, Olguin M, Spear CE, Leiter KW, Knap J. Towards high throughput screening of electrochemical stability of battery electrolytes. Nanotechnology. 2015d;26.

Borodin O, Olguin M, Spear CE, Leiter KW, Knap J, Yushin G, Childs AS, Xu K. Challenges with quantum chemistry-based screening of electrochemical stability of lithium battery electrolytes. Symposium on Batteries - Theory, Modeling, and Simulation - 228th ECS Meeting. ECS Transactions; 2015.

Borodin O, Price DL, Aoun B, Gonzalez MA, Hooper JB, Kofu M, Kohara S, Yamamuro O, Saboungi M-L. Effect of water on the structure of a prototype ionic liquid. Phys Chem Chem Phys. 2016b;18:23474–23481.

Borodin O, Ren X, Vatamanu J, Von Wald Cresce A, Knap J, Xu K. Modeling insight into battery electrolyte electrochemical stability and interfacial structure. Acc Chem Res. 2017a;50:2886–2894.

Borodin O, Self J, Persson KA, Wang C, Xu K. Uncharted waters: super-concentrated electrolytes. Joule. 2020;4:69–100.

Borodin O, Suo L, Gobet M, Ren X, Wang F, Faraone A, Peng J, Olguin M, Schroeder M, Ding MS, et al. Liquid structure with nano-heterogeneity promotes cationic transport in concentrated electrolytes. ACS Nano. 2017b;11:10462–10471.

Cao C, Pollard TP, Borodin O, Mars JE, Tsao Y, Lukatskaya MR, Kasse RM, Schroeder MA, Xu K, Toney MF, et al. Toward unraveling the origin of lithium fluoride in the solid electrolyte interphase. Chem Mater. 2021a;33:7315–7336.

Cao L, Li D, Pollard T, Deng T, Zhang B, Yang C, Chen L, Vatamanu J, Hu E, Hourwitz MJ, et al. Fluorinated interphase enables reversible aqueous zinc battery chemistries. Nature Nanotechnology. 2021b;16:902–910.

Carlin C, Rinderspacher BC. Twist rotation of (0001) gallium nitride on (0001) 6H-silicon carbide substrate. CCDC Army Research Laboratory; 2019. Report No.: ARL-TR-8868.

Carlin CM, Rinderspacher BC. ARL_Transire. Army Research Laboratory (US); n.d. https://github.com/USArmyResearchLab/ARL_Transire.

Carlin CM, Rinderspacher BC. Transire, a program for generating solid-state interface structures. CCDC Army Research Laboratory; 2017. Report No.: ARL-TR-8134.

Carter WJ and Marsh, SP. Hugoniot equation of state of polymers. Los Alamos National Laboratory; 1995.

Chantawansri TL, Sirk TW, Byrd EFC, Andzelm JW, Rice BM. Shock Hugoniot calculations of polymers using quantum mechanics and molecular dynamics. Journal of Chemical Physics. 2012;137.

Chapman N, Borodin O, Yoon T, Nguyen CC, Lucht BL. Spectroscopic and density functional theory characterization of common lithium salt solvates in carbonate electrolytes for lithium batteries. J Phys Chem C. 2017;121:2135–2148.

Chen J, Fan X, Li Q, Yang H, Khoshi MR, Xu Y, Hwang S, Chen L, Ji X, Yang C, et al. Electrolyte design for LiF-rich solid–electrolyte interfaces to enable high-performance microsized alloy anodes for batteries. Nature Energy; 2020a;5:386–397.

Chen J, Li Q, Pollard TP, Fan X, Borodin O, Wang C. Electrolyte design for Li metal-free Li batteries. Materials Today. 2020b;39:118–126.

Chen J, Vatamanu J, Xing L, Borodin O, Chen H, Guan X, Liu X, Xu K, Li W. Improving electrochemical stability and low-temperature performance with water/acetonitrile hybrid electrolytes. Adv Energ Mater. 2020c;10:1902654.

Chen L, Zhang J, Li Q, Vatamanu J, Ji X, Pollard TP, Cui C, Hou S, Chen J, Yang C, et al. A 63 m superconcentrated aqueous electrolyte for high-energy Li-ion batteries. ACS Energy Lett. 2020d;5:968–974.

Cho J, Crone JC, Arsenlis A, Aubry S. Dislocation dynamics in polycrystalline materials. Modelling and Simulation in Materials Science and Engineering. 2020a;28.

Cho S-J, Yu D-E, Pollard TP, Moon H, Jang M, Borodin O, Lee S-Y. Nonflammable lithium metal full cells with ultra-high energy density based on coordinated carbonate electrolytes. iScience. 2020b;23:100844.

Cortona P. Self-consistently determined properties of solids without band-structure calculations. Physical Review B. 1991;44:8454–8458.

Cresce AV, Russell SM, Borodin O, Allen JA, Schroeder MA, Dai M, Peng J, Gobet MP, Greenbaum SG, Rogers RE, et al. Solvation behavior of carbonate-based electrolytes in sodium ion batteries. Phys Chem Chem Phys. 2017;19:574–586.

Crone JC, Chung PW, Leiter KW, Knap J, Aubry S, Hommes G, Arsenlis A. A multiply parallel implementation of finite element-based discrete dislocation dynamics for arbitrary geometries. Modelling and Simulation in Materials Science and Engineering. 2014;22.

Crone JC, Leiter KW, Knap J. Finite Element for Discrete Dislocation Dynamics (FED3) user guide. DEVCOM Army Research Laboratory; 2021. Report No.: ARL-TR-9255.

Crone JC, Munday LB. Knap J. Capturing the effects of free surfaces on void strengthening with dislocation dynamics. Acta Materialia. 2015;101:40–47.

Crone JC, Munday LB, Ramsey JJ, Knap J. Modeling the effect of dislocation density on the strength statistics in nanoindentation. Modelling and Simulation in Materials Science and Engineering. 2018;26.

Crone JC, Munday LB. Parallel performance of linear solvers and preconditioners. Army Research Laboratory (US); 2014. Report No.: ARL-TR-6778.

Davies DM, Yang Y, Sablina ES, Yin Y, Mayer M, Zhang Y, Olguin M, Lee JZ, Lu B, Damien D, et al. A Safer, wide-temperature liquefied gas electrolyte based on difluoromethane. J Power Sources. 2021;493:229668.

Delp SA, Borodin O, Olguin M, Eisner CG, Allen JL, Jow TR. Importance of reduction and oxidation stability of high voltage electrolytes and additives. Electrochimica Acta. 2016;209:498–510.

Deng M, Li Z, Borodin O, Karniadakis GE. cDPD: a new dissipative particle dynamics method for modeling electrokinetic phenomena at the mesoscale. J Chem Phys. 2016;145:144109.

Elstner M, Porezag D, Jungnickel G, Elsner J, Haugk M, Frauenheim T, Suhai S, Seifert G. Self-consistent-charge density-functional tight-binding method for simulations of complex materials properties. Physical Review B. 1998;58:7260–7268.

Falgout RD, Yang UM. HYPRE: A library of high performance preconditioners. Proceedings Computational Science-ICCS; 2002. Pt Iii;2331:632–641.

Fan X, Chen L, Borodin O, Ji X, Chen J, Hou S, Deng T, Zheng J, Yang C, Liou S. C, et al. Non-flammable electrolyte enables Li-metal batteries with aggressive cathode chemistries. Nat Nanotech. 2018;13:715–722.

Gavini V, Bhattacharya K, Ortiz M. Quasi-continuum orbital-free density-functional theory: A route to multi-million atom non-periodic DFT calculation. Journal of the Mechanics and Physics of Solids. 2007;55:697–718.

Geiculescu OE, Hallac BB, Rajagopal RV, Creager SE, Desmarteau DD, Borodin O, Smith GD. The effect of low-molecular-weight poly(ethylene glycol) (PEG) plasticizers on the transport properties of lithium fluorosulfonimide ionic melt electrolytes. J Phys Chem B. 2014;118:5135–5143.

Glaser R, Borodin O, Johnson BR, Jhulki S, Yushin G. Minimizing long-chain polysulfide formation in Li-S batteries by using localized low concentration highly fluorinated electrolytes. J Electrochem Soc. 2021.

González MA, Borodin O, Kofu M, Shibata K, Yamada T, Yamamuro O, Xu K, Price DL, Saboungi M-L. Nanoscale relaxation in “water-in-salt” and “water-in-bisalt” electrolytes. J Phys Chem Lett. 2020;7279–7284.

Gonze X, Amadon B, Antonius G, Arnardi F, Baguet L, Beuken J-M, Bieder J, Bottin F, Bouchet J, Bousquet E, et al. The Abinitproject: impact, environment and recent developments. Computer Physics Communications. 2020;248:107042.

Goodpaster JD, Ananth N, Manby FR, Miller TF. Exact nonadditive kinetic potentials for embedded density functional theory. Journal of Chemical Physics. 2010;133.

Goodpaster JD, Barnes TA, Miller TF. Embedded density functional theory for covalently bonded and strongly interacting subsystems. Journal of Chemical Physics. 2011;134.

Govind N, Wang YA, Da Silva AJR, Carter EA. Accurate ab initio energetics of extended systems via explicit correlation embedded in a density functional environment. Chemical Physics Letters. 1998;295:129–134.

Groen D, Knap J, Neumann P, Suleimenova D, Veen L, Leiter K. Mastering the scales: a survey on the benefits of multiscale computing software. Philosophical Transactions of the Royal Society a-Mathematical Physical and Engineering Sciences. 2019;377.

Gu W, Borodin O, Zdyrko B, Lin H-T, Kim H, Nitta N, Huang J, Magasinski A, Milicev Z, Berdichevsky G et al. Conversion cathodes: lithium–iron fluoride battery with in situ surface protection. Adv Funct Mater. 2016 Oct;26:1490–1490.

Han S-D, Borodin O, Seo DM, Zhou Z-B, Henderson WA. Electrolyte solvation and ionic association: v. acetonitrile-lithium bis(fluorosulfonyl)imide (LiFSI) mixtures. J Electrochem Soc. 2014;161:A2042–A2053.

Han SD, Yun SH, Borodin O, Seo DM, Sommer RD, Young VG, Henderson WA. Solvate structures and computational/spectroscopic characterization of $LiPF_6$ electrolytes. J Phys Chem C. 2015;119:8492–8500.

Harrison RJ. Krylov subspace accelerated inexact Newton method for linear and nonlinear equations. Journal of Computational Chemistry. 2004;25:328–334.

Haskins JB, Bennett WR, Wu JJ, Hernández DM, Borodin O, Monk JD, Bauschlicher CW, Lawson JW. Computational and experimental investigation of Li-doped ionic liquid electrolytes: [pyr14][TFSI], [pyr13][FSI], and [EMIM][BF_4]. J Phys Chem B. 2014;118:11295–11309.

He Y, Qiao R, Vatamanu J, Borodin O, Bedrov D, Huang J, Sumpter BG. Importance of ion packing on the dynamics of ionic liquids during micropore charging. J Phys Chem Lett. 2016;7:36–42.

Henderson WA, Seo DM, Han S-D, Borodin O. Electrolyte solvation and ionic association. VII. correlating Raman spectroscopic data with solvate species. J Electrochem Soc. 2020;167:110551.

Ho JS, Borodin OA, Ding MS, Ma L, Schroeder MA, Pastel GR, Xu K. Understanding lithium-ion transport in sulfolane- and tetraglyme-based electrolytes using very low frequency impedance spectroscopy. Energy & Environmental Materials. 2021.

Hou S, Ji X, Gaskell K, Wang P-F, Wang L, Xu J, Sun R, Borodin O, Wang C. Solvation sheath reorganization enables divalent metal batteries with fast interfacial charge transfer kinetics. Science. 2021a;374:172–178.

Hou X, Pollard TP, Zhao W, He X, Ju X, Wang J, Du L, Paillard E, Lin H, Xu K, Borodin O, Winter M et al. Simultaneous formation of interphases on both positive and negative electrodes in high-voltage aqueous lithium-ion batteries. Small. 2021b;2104986.

Hou X, Wang R, He X, Pollard TP, Ju X, Du L, Paillard E, Frielinghaus H, Barnsley LC, Borodin O, et al. Stabilizing the solid-electrolyte interphase with polyacrylamide for high-voltage aqueous lithium-ion batteries. Angew Chem Int Ed. 2021c;60:22812–22817.

Hourahine B, Aradi B, Blum V, Bonafé F, Buccheri A, Camacho C, Cevallos C, Deshaye My, Dumitrică T, Dominguez A, et al. DFTB+, a software package for efficient approximate density functional theory based atomistic simulations. The Journal of Chemical Physics. 2020;152:124101.

Hu Z, Vatamanu J, Borodin O, Bedrov D. A comparative study of alkylimidazolium room temperature ionic liquids with FSI and TFSI anions near charged electrodes. Electrochimica Acta. 2014;145:40–52.

Huang Q, Pollard TP, Ren X, Kim D, Magasinski A, Borodin O, Yushin G. Fading mechanisms and voltage hysteresis in FeF_2–NiF_2 solid solution cathodes for lithium and lithium-ion batteries. Small. 2019:1804670–10.

Islam MM, Ostadhossein A, Borodin O, Yeates AT, Tipton WW, Hennig RG, Kumar N, Van Duin ACT. ReaxFF molecular dynamics simulations on lithiated sulfur cathode materials. Phys Chem Chem Phys. 2015;17:3383–3393.

Jiang L, Liu L, Yue J, Zhang Q, Zhou A, Borodin O, Suo L, Li H, Chen L, Xu K, et al. High-voltage aqueous Na-ion battery enabled by inert-cation-assisted water-in-salt electrolyte. Adv Mater. 2020;32:1904427.

Jones KA, Batyrev IG. The structure of dislocations in (In,Al,Ga)N wurtzite films grown epitaxially on (0001) or (11(2)over-bar2) GaN or AlN substrates. Journal of Applied Physics. 2012;112.

Jow TR, Allen JL, Borodin OA, Delp SA, Allen JL. Challenges in developing high energy density Li-ion batteries with high voltage cathodes. TMS 2014 Supplemental Proceedings. John Wiley & Sons, Inc; 2014.

Kanungo B, Gavini V. Large-scale all-electron density functional theory calculations using an enriched finite-element basis. Physical Review B. 2017;95.

Kanungo B, Gavini V. Real time time-dependent density functional theory using higher order finite-element methods. Physical Review B. 2019;100.

Kim C, Borodin O, Karniadakis GE. Quantification of sampling uncertainty for molecular dynamics simulation: time-dependent diffusion coefficient in simple fluids. J Comput Phys. 2015a;302:485–508.

Kim H, Wu F, Lee JT, Nitta N, Lin H-T, Oschatz M, Cho WI, Kaskel S, Borodin O, Yushin G. In situ formation of protective coatings on sulfur cathodes in lithium batteries with LiFSI-based organic electrolytes. Adv Energy Mater. 2015b;5:1401792.

Knap J, Barton NR, Hornung RD, Arsenlis A, Becker R, Jefferson DR. Adaptive sampling, in hierarchical simulation. International Journal for Numerical Methods in Engineering. 2008;76:572–600.

Knap J, Spear C, Leiter K, Becker R, Powell D. A computational framework for scale-bridging in multi-scale simulations. International Journal for Numerical Methods in Engineering. 2016;108:1649– 1666.

Knap J, Spear CE, Borodin O, Leiter KW. Advancing a distributed multi-scale computing framework for large-scale high-throughput discovery in materials science. Nanotechnology. 2015;26:434004.

Kresse G, Furthmüller J. Efficient iterative schemes for ab initio total-energy calculations using a plane-wave basis set. Physical Review B. 1996;54:11169–11186.

Krimsky E, Jones KA, Tompkins RP, Rotella P, Ligda J, Schuster BE. Nano-indentation used to study pyramidal slip in GaN single crystals. Journal of Applied Physics. 2018;123.

Kuhne TD, Iannuzzi M, Del Ben M, Rybkin VV, Seewald P, Stein F, Laino T, Khaliullin RZ, Schutt O, Schiffmann F, et al. CP2K: an electronic structure and molecular dynamics software package – Quickstep: efficient and accurate electronic structure calculations. Journal of Chemical Physics. 2020;152.

Lee M, Leiter K, Eisner C, Crone J, Knap J. Extended Huckel and Slater's rule initial guess for real space grid-based density functional theory. Computational and Theoretical Chemistry. 2015;1062:24–29.

Leiter KW, Barnes BC, Becker R, Knap J. Accelerated scale-bridging through adaptive surrogate model evaluation. Journal of Computational Science. 2018;27:91–106.

Leiter KW, Crone JC, Knap J. An algorithm for massively parallel dislocation dynamics simulations of small scale plasticity. Journal of Computational Science. 2013;4L:401–411.

Leiter KW, Larentzos JP, Barnes BC, Brennan JK, Becker R, Knap J. Temporal scale-bridging of chemistry in a multiscale model of a reacting energetic material. Journal of Computational Physics. Forthcoming 2022, under review.

Lesch V, Jeremias S, Moretti A, Passerini S, Heuer A, Borodin O. A combined theoretical and experimental study of the influence of different anion ratios on lithium ion dynamics in ionic liquids. J Phys Chem B. 2014;118:7367–7375.

Lesch V, Li Z, Bedrov D, Borodin O, Heuer A. The influence of cations on lithium ion coordination and transport in ionic liquid electrolytes: a MD simulation study. Phys Chem Chem Phys. 2016;18:382–392.

Li Z, Borodin O, Smith GD, Bedrov D. Effect of organic solvents on Li^+ ion solvation and transport in ionic liquid electrolytes: a molecular dynamics simulation study. J Phys Chem B. 2015;119:3085–3096.

Li Z, Bouchal R, Mendez-Morales T, Rollet AL, Rizzi C, Le Vot S, Favier F, Rotenberg B, Borodin O, Fontaine O, et al. Transport properties of Li-TFSI water-in-salt electrolytes. J Phys Chem C. 2019;123:10514–10521.

Lísal M, Larentzos JP, Sellers MS, Schweigert IV, Brennan JK. Dissipative particle dynamics with reactions: Application to RDX decomposition. Journal of Chemical Physics. 2019;151.

Liu YF, Raghothamachar B, Peng HY, Ailihumaer T, Dudley M, Collazo R, Tweedie J, Sitar Z, Shahedipour-Sandvik FS, Jones KA, et al. Synchrotron X-ray topography characterization of high quality ammonothermal-grown gallium nitride substrates. Journal of Crystal Growth. 2020;551.

Lu DP, Tao JH, Yan PF, Henderson WA, Li QY, Shao YY, Helm ML, Borodin O, Graff GL, Polzin B, et al. Formation of reversible solid electrolyte interface on graphite surface from concentrated electrolytes. Nano Letters. 2017;17:1602–1609.

Luo C, Borodin O, Ji X, Hou S, Gaskell Kj, Fan X, Chen J, Deng T, Wang R, Jiang J, et al. Azo compounds as a family of organic electrode materials for alkali-ion batteries. Proc Natl Acad Sci. 2018;115:2004–2009.

Luo C, Zhu Y, Borodin O, Gao T, Fan X, Xu Y, Xu K, Wang C. Activation of oxygen-stabilized sulfur for Li and Na batteries. Adv Func Mater. 2016;26:745–752.

Ma L, Lee JZ, Pollard TP, Schroeder MA, Limpert MA, Craven B, Fess S, Rustomji CS, Wang C, Borodin O, et al. High-efficiency zinc-metal anode enabled by liquefied gas electrolytes. ACS Energy Letters. 2021a:4426–4430.

Ma L, Pollard TP, Zhang Y, Schroeder MA, Ding MS, Cresce AV, Sun R, Baker DR, Helms BA, Maginn EJ, et al. Functionalized phosphonium cations enable zinc metal reversibility in aqueous electrolytes. Angew. Chem Int Ed. 2021b;60:12438–12445.

Ma L, Schroeder MA, Borodin O, Pollard TP, Ding MS, Wang C, Xu K. Realizing high zinc reversibility in rechargeable batteries. Nature Energy. 2020a;5:743–749.

Ma L, Schroeder MA, Pollard TP, Borodin O, Ding MS, Sun R, Cao L, Ho J, Baker DR, Wang C, Xu K. Critical factors dictating reversibility of the zinc metal anode. Energy & Environmental Materials. 2020b.

Mallick DD, Prameela SE, Ozturk D, Williams CL, Kang MJ, Valentino GM, Lloyd JT, Wilkerson JW, Weihs TP, Ramesh KT. Spall strength in alloyed magnesium: a compendium of research efforts from the CMEDE 10-year effort. Mechanics of Materials. 2021;162.

Mao M, Luo C, Pollard TP, Hou S, Gao T, Fan X, Cui C, Yue J, Tong Y, Yang G, et al. A pyrazine-based polymer for fast-charge batteries. Angew Chem Int Ed. 2019;58:17820–17826.

Mcclure JP, Borodin O, Olguin M, Chu D, Fedkiw PS. Sensitivity of density functional theory methodology for oxygen reduction reaction predictions on Fe–N_4-containing graphitic clusters. J Phys Chem C. 2016;120:28545–28562.

Mcowen DW, Seo DM, Borodin O, Vatamanu J, Boyle PD, Henderson WA. Concentrated electrolytes: decrypting electrolyte properties and reassessing Al corrosion mechanisms. Ener Env Sci. 2014;7:416–426.

Mogurampelly S, Borodin O, Ganesan V. Computer simulations of ion transport in polymer electrolyte membranes. Annu Rev Chem Biomol Eng. 2016;7:349–371.

Motamarri P, Das S, Rudraraju S, Ghosh K, Davydov D, Gavini V. DFT-FE - A massively parallel adaptive finite-element code for large-scale density functional theory calculations. Computer Physics Communications. 2020;246.

Motamarri P, Gavini V. Configurational forces in electronic structure calculations using Kohn-Sham density functional theory. Physical Review B. 2018;97.

Motamarri P, Nowak MR, Leiter K, Knap J, Gavini V. Higher-order adaptive finite-element methods for Kohn–Sham density functional theory. Journal of Computational Physics. 2013;253:308–343.

Mullin J. Trace conserving purification for linear scaling [O(N)] methods: a first enhancement to CP2K. Army Research Laboratory (US); 2014. Report No.: ARL-CR-0746.

Munday LB, Crone JC, Knap J. The role of free surfaces on the formation of prismatic dislocation loops. Scripta Materialia. 2015;103:65–68.

Munday LB, Crone JC, Knap J. Prismatic and helical dislocation loop generation from defects. Acta Materialia. 2016;103:217–228.

Niklasson AMN. Extended Born-Oppenheimer molecular dynamics. Physical Review Letters. 2008;100.

Niklasson AMN, Steneteg P, Odell A, Bock N, Challacombe M, Tymczak CJ, Holmström E, Zheng G, Weber V. Extended Lagrangian Born–Oppenheimer molecular dynamics with dissipation. Journal of Chemical Physics. 2009;130:214109.

Olivier A, Giovanis DG, Aakash BS, Chauhan M, Vandanapu L, Shields MD. UQpy: a general purpose Python package and development environment for uncertainty quantification. Journal of Computational Science. 2020;47.

Peng J, Gobet M, Devany M, Xu K, Cresce AVW, Borodin O, Greenbaum S. Multinuclear magnetic resonance investigation of cation-anion and anion-solvent interactions in carbonate electrolytes. J Power Sources. 2018;399:215–222.

Perdew JP, Burke K, Ernzerhof M. Generalized gradient approximation made simple. Physical Review Letters. 1996;77:3865–3868.

Perdew JP, Burke K. Ernzerhof M. Generalized gradient approximation made simple (erratum). Physical Review Letters. 1997;78:1396–1396.

Price DL, Borodin O, González MA, Kofu M, Shibata K, Yamada T, Yamamuro O, Saboungi M-L. Relaxation in a prototype ionic liquid: influence of water on the dynamics. J Phys Chem Lett. 2017;715–719.

Pulay P. Convergence acceleration of iterative sequences. the case of SCF iteration. Chemical Physics Letters. 1980;73:393–398.

Pulay P. Improved SCF convergence acceleration. Journal of Computational Chemistry. 1982;3:556–560.

Qian J, Henderson WA, Xu W, Bhattacharya P, Engelhard M, Borodin O, Zhang J-G. High rate and stable cycling of lithium metal anode. Nat Commun. 2015;6:6362.

Raberg JH, Vatamanu J, Harris SJ, Van Oversteeg CHM, Ramos A, Borodin O, Cuk T. Probing electric double-layer composition via in situ vibrational spectroscopy and molecular simulations. J Phys Chem Lett. 2019;10:3381–3389.

Seo DM, Boyle PD, Sommer RD, Daubert JS, Borodin O, Henderson WA. Solvate structures and spectroscopic characterization of LiTFSI electrolytes. J Phys Chem B. 2014;118:13601–13608.

Shadike Z, Lee H, Borodin O, Cao X, Fan X, Wang X, Lin R, Bak S-M, Ghose S, Xu K, et al. Identification of LiH and nanocrystalline LiF in the solid–electrolyte interphase of lithium metal anodes. Nature Nanotechnology. 2021;16:549–554.

Smith JW, Lam RK, Sheardy AT, Shih O, Rizzuto AM, Borodin O, Harris SJ, Prendergast D, Saykally RJ. X-ray absorption spectroscopy of $LiBF_4$ in propylene carbonate: a model lithium ion battery electrolyte. Phys Chem Chem Phys. 2014;16:23568–23575.

Song A-Y, Turcheniuk K, Leisen J, Xiao Y, Meda L, Borodin O, Yushin G. Understanding Li-ion dynamics in lithium hydroxychloride (Li_2OHCl) solid state electrolyte via addressing the role of protons. Adv Energ Mater. 2020;10:1903480.

Song AY, Xiao YR, Turcheniuk K, Upadhya P, Ramanujapuram A, Benson J, Magasinski A, Olguin M, Meda L, Borodin O, et al. Protons enhance conductivities in lithium halide hydroxide/lithium oxyhalide solid electrolytes by forming rotating hydroxy groups. Adv Energ Mater. 2018;8:1700971–1700978.

Soumagne J, Biddiscombe J, Clarke J. An HDF5 MPI virtual file driver for parallel in-situ post-processing. Recent Advances in the Message Passing Interface. 2010;6305:62–+.

Steinrück H-G, Cao C, Lukatskaya MR, Takacs CJ, Wan G, Mackanic DG, Tsao Y, Zhao J, Helms BA, Xu K, et al. Interfacial speciation determines interfacial chemistry: X-ray-induced lithium fluoride formation from water-in-salt electrolytes on solid surfaces. Angew Chem Int Ed. 2020a;59:23180–23187.

Steinrück H-G, Cao C, Tsao Y, Takacs CJ, Konovalov O, Vatamanu J, Borodin O, Toney MF. The nanoscale structure of the electrolyte–metal oxide interface. Ener Env Sci. 2018;11:594–602.

Steinrück H-G, Takacs CJ, Kim H-K, Mackanic DG, Holladay B, Cao C, Narayanan S, Dufresne EM, Chushkin Y, Ruta B, et al. Concentration and velocity profiles in a polymeric lithium-ion battery electrolyte. Energy Environ Sci. 2020b;13:4312–4321.

Suo L, Borodin O, Gao T, Olguin M, Ho J, Fan X, Luo C, Wang C, Xu K. "Water-in-salt" electrolyte enables high-voltage aqueous lithium-ion chemistries. Science. 2015;350:938–943.

Suo L, Borodin O, Sun W, Fan X, Yang C, Wang F, Gao T, Ma Z, Schroeder M, Von Cresce A, et al. Advanced high-voltage aqueous lithium-ion battery enabled by "water-in-bisalt" electrolyte. Angew Chem Int Ed. 2016;55:7136–7141.

Suo L, Borodin O, Wang Y, Rong X, Sun W, Fan X, Xu S, Schroeder MA, Cresce AV, Wang F, et al. "Water-in-salt" electrolyte makes aqueous sodium-ion battery safe, green, and long-lasting. Adv Energy Mater. 2017a;1701189.

Suo L, Oh D, Lin Y, Zhuo Z, Borodin O, Gao T, Wang F, Kushima A, Wang Z, Kim H-C, et al. How solid-electrolyte interphase forms in aqueous electrolytes. J Am Chem Soc. 2017b;139:18670–18680.

Suryanarayana P. Optimized purification for density matrix calculation. Chemical Physics Letters. 2013;555:291–295.

Szajewski BA, Crone JC, Knap J. Analytic model for the line tension of a bowing dislocation segment. Philosophical Magazine Letters. 2019;99:77–86.

Szajewski BA, Crone JC, Knap J. Analytic model for the Orowan dislocation-precipitate bypass mechanism. Materialia. 2020;11:100671.

Szajewski BA, Crone JC, Knap J. Dislocation precipitate bypass through elastically mismatched precipitates. Modelling and Simulation in Materials Science and Engineering. 2021;29.

Szajewski BA, Crone JC, Knap J. Statistical modeling of the Orowan bypass mechanism for randomly distributed obstacles. Physical Review Materials. Forthcoming 2022, submitted.

Thompson AP, Aktulga HM, Berger R, Bolintineanu DS, Brown WM, Crozier PS, In 'T Veld PJ, Kohlmeyer A, Moore SG, Nguyen TD, et al. LAMMPS – a flexible simulation tool for particle-based materials modeling at the atomic, meso, and continuum scales. Computer Physics Communications. 2022;271:108171.

Vatamanu J, Bedrov D, Borodin O. On the application of constant electrode potential simulation techniques in atomistic modelling of electric double layers. Molecular Simulation. 2017a;43:838–849.

Vatamanu J, Borodin O. Ramifications of water-in-salt interfacial structure at charged electrodes for electrolyte electrochemical stability. J Phys Chem Lett. 2017;8:4362–4367.

Vatamanu J, Borodin O, Bedrov D. Application of screening functions as cut-off based alternative to Ewald summation in molecular dynamics simulations using polarizable force fields. J Chem Theory and Comput. 2018;14:768–783.

Vatamanu J, Borodin O, Olguin M, Yushin G, Bedrov D. Charge storage at the nanoscale: understanding the trends from the molecular scale perspective. J Mater Chem A. 2017b;5:21049–21076.

Vatamanu J, Borodin O, Smith GD. Molecular dynamics simulation studies of the structure of a mixed carbonate/$LiPF_6$ electrolyte near graphite surface as a function of electrode potential. J Phys Chem C. 2012;116:1114–1121.

Vatamanu J, Vatamanu M, Borodin O, Bedrov D. A comparative study of room temperature ionic liquids and their organic solvent mixtures near charged electrodes. J Phys Condensed Matter. 2016;28:464002.

Von Aspern N, Grünebaum M, Diddens D, Pollard T, Wölke C, Borodin O, Winter M, Cekic-Laskovic I. Methyl-group functionalization of pyrazole-based additives for advanced lithium ion battery electrolytes. J Power Sources. 2020;461:228159.

Von Wald Cresce A, Gobet M, Borodin O, Peng J, Russell SM, Wikner E, Fu A, Hu L, Lee H-S, Zhang Z, et al. Anion solvation in carbonate-based electrolytes. J Phys Chem C. 2015;119:27255–27264.

Wan C, Hu MY, Borodin O, Qian J, Qin Z, Zhang J-G, Hu JZ. Natural abundance ^{17}O, ^{6}Li NMR and molecular modeling studies of the solvation structures of lithium bis(fluorosulfonyl)imide/1,2-dimethoxyethane liquid electrolytes. J Power Sources. 2016;307:231–243.

Wang F, Borodin O, Ding MS, Gobet M, Vatamanu J, Fan X, Gao T, Edison N, Liang Y, Sun W, et al. Hybrid aqueous/non-aqueous electrolyte for safe and high-energy Li-ion batteries. Joule. 2018a;2:927–937.

Wang F, Borodin O, Gao T, Fan X, Sun W, Han F, Faraone A, Dura JA, Xu K, Wang C. Highly reversible zinc metal anode for aqueous batteries. Nat Mater. 2018b;17:543–549.

Wang L, Menakath A, Han F, Wang Y, Zavalij PY, Gaskell KJ, Borodin O, Iuga D, Brown SP, Wang C, et al. Identifying the components of the solid–electrolyte interphase in Li-ion batteries. Nat Chem. 2019;11:789–796.

Wang YT, Xing LD, Borodin O, Huang WN, Xu MQ, Li XP, Li WS. Quantum chemistry study of the oxidation-induced stability and decomposition of propylene carbonate-containing complexes. Phys Chem Chem Phys. 2014;16:6560–6567.

Weingarten NS. Dislocation mobilities in GaN from molecular dynamics simulations. MRS Online Proceedings Library. 2015;1741:1–6.

Weingarten NS. Dislocation mobility and Peierls stress of c-type screw dislocations in GaN from molecular dynamics. Computational Materials Science. 2018;153:409–416.

Weingarten NS, Chung PW. a-Type edge dislocation mobility in wurtzite GaN using molecular dynamics. Scripta Materialia. 2013;69:311–314.

Weingarten NS, Larentzos JP. Implementation of shifted periodic boundary conditions in the large-scale atomic/molecular massively parallel simulator (LAMMPS) software. Army Research Laboratory (US); 2015. Report No.: ARL-TN-0687.

Wesołowski TA. One-electron equations for embedded electron density: challenge for theory and practical payoffs in multi-level modelling of complex polyatomic systems. computational chemistry: reviews of current trends. World Scientific. 2006.

Wesolowski TA, Warshel A. Frozen density functional approach for ab initio calculations of solvated molecules. Journal of Physical Chemistry. 1993;97:8050–8053.

Widstrom MD, Borodin O, Ludwig KB, Matthews JE, Bhattacharyya S, Garaga MV, Cresce A, Jarry A, Erdi M, Wang C, et al. Water domain enabled transport in polymer electrolytes for lithium-ion batteries. Macromolecules. 2021;54:2882–2891.

Wu C-C, Aubry S, Chung PW, Arsenlis A. Dislocation dynamics simulations of junctions in hexagonal close-packed crystals. MRS Proceedings. 2012;1424:mrsf11-1424-ss07-37.

Wu CC, Aubry S, Arsenlis A, Chung PW. Binary dislocation junction formation and strength in hexagonal close-packed crystals. International Journal of Plasticity. 2016;79:176–195.

Wu CC, Chung PW, Aubry S, Munday LB, Arsenlis A. The strength of binary junctions in hexagonal close-packed crystals. Acta Materialia. 2013;61:3422–3431.

Wu CC, Weingarten NS, Chung PW. Cross slip of dislocation loops in GaN under shear. Physica Status Solidi C: Current Topics in Solid State Physics. 2014;11(3–4):432–436.

Wu F, Borodin O, Yushin G. In situ surface protection for enhancing stability and performance of conversion-type cathodes. MRS Energy & Sustainability. 2017a;4:1–15.

Wu F, Chu F, Ferrero GA, Sevilla M, Fuertes AB, Borodin O, Yu Y, Yushin G. Boosting high-performance in lithium–sulfur batteries via dilute electrolyte. Nano Lett. 2020;20:5391–5399.

Wu F, Lee JT, Nitta N, Kim H, Borodin O, Yushin G. Lithium iodide as a promising electrolyte additive for lithium–sulfur batteries: mechanisms of performance enhancement. Adv Mater. 2015;27:101–108.

Wu F, Pollard TP, Zhao E, Xiao Y, Olguin M, Borodin O, Yushin G. Layered $LiTiO_2$ for the protection of Li_2S cathodes against dissolution: mechanisms of the remarkable performance boost. Ener Env Sci. 2018;11:807–817.

Wu F, Thieme S, Ramanujapuram A, Zhao E, Weller C, Althues H, Kaskel S, Borodin O, Yushin G. Toward in-situ protected sulfur cathodes by using lithium bromide and pre-charge. Nano Energy. 2017b;40:170–179.

Yang C, Chen J, Ji X, Pollard TP, Lü X, Sun C-J, Hou S, Liu Q, Liu C, Qing T, et al. Aqueous Li-ion battery enabled by halogen conversion–intercalation chemistry in graphite. Nature. 2019a;569:245–250.

Yang C, Chen J, Qing T, Fan X, Sun W, Von Cresce A, Ding MS, Borodin O, Vatamanu J, Schroeder MA, et al. 4.0 V Aqueous Li-ion batteries. Joule. 2017a;1:122–132.

Yang C, Suo L, Borodin O, Wang F, Sun W, Gao T, Fan X, Hou S, Ma Z, Amine K, et al. Unique aqueous Li-ion/sulfur chemistry with high energy density and reversibility. Proc Natl Acad Sci. 2017b;114:6197–6202.

Yang Y, Davies DM, Yin Y, Borodin O, Lee JZ, Fang C, Olguin M, Zhang Y, Sablina ES, Wang X, Rustomji CS, et al. High-efficiency lithium-metal anode enabled by liquefied gas electrolytes. Joule. 2019b;3:1986–2000.

Yang Y, Yin Y, Davies DM, Zhang M, Mayer M, Zhang Y, Sablina ES, Wang S, Lee JZ, Borodin O, et al. Liquefied gas electrolytes for wide-temperature lithium metal batteries. Energy Environ Sci. 2020;13:2209–2219.

Zhang S, Pollard TP, Feng X, Borodin O, Xu K, Li Z. Altering the electrochemical pathway of sulfur chemistry with oxygen for high energy density and low shuttling in a Na/S battery. ACS Energy Lett. 2020;1070–1076.

Zhang Y, Su M, Yu X, Zhou Y, Wang J, Cao R, Xu W, Wang C, Baer DR, Borodin O, et al. Investigation of ion–solvent interactions in nonaqueous electrolytes using in situ liquid SIMS. Analytical Chemistry. 2018;90:3341–3348.

Zhang Y, Wan G, Lewis NHC, Mars J, Bone SE, Steinrück H-G, Lukatskaya MR, Weadock NJ, Bajdich M, et al. Water or anion? uncovering the Zn^{2+} solvation environment in mixed $Zn(TFSI)_2$ and LiTFSI water-in-salt electrolytes. ACS Energy Letters. 2021;3458–3463.

Zhao E, Borodin O, Gao X, Lei D, Xiao Y, Ren X, Fu W, Magasinski A, Turcheniuk K, Yushin G. Lithium–iron (III) fluoride battery with double surface protection. Advanced Energy Materials. 2018;1800721.

Zhou Y, Su M, Yu X, Zhang Y, Wang J-G, Ren X, Cao R, Xu W, Baer DR, Du Y, et al. Real-time mass spectrometric characterization of the solid–electrolyte interphase of a lithium-ion battery. Nat Nanotechnol. 2020;15:224–230.

List of Symbols, Abbreviations, and Acronyms

ABAQUS	software suite for FE analysis and computer-aided engineering
ABINIT	software suite for DFT calculations of materials
ALE3D	LLNL multiphysics simulation tool
ALEGRA	Sandia National Laboratory's shock and multiphysics family of codes
AMG	algebraic multigrid
APPLE&P	Atomistic Polarizable Potential for Liquids, Electrolytes, and Polymers
ARL	Army Research Laboratory
B3LYP	Becke, 3-parameter, Lee–Yang–Parr
BCC	body-centered cubic
BOMD	Born–Oppenheimer molecular dynamics
CCSD(T)	coupled cluster method with a full treatment singles and doubles in describing many-body systems
CP2K	quantum chemistry and solid-state physics software package
CPU	central processing unit
CRA	Collaborative Research Alliance
DDD	discrete dislocation dynamics
DEVCOM	US Army Combat Capabilities Development Command
DFT	density functional theory
DFTB	tight-binding DFT
DFTB+	software package that implements the DFTB method
DFT-FE	efficient and massively parallel FE code for large-scale DFT calculations
DIIS	Direct Inversion in the Iterative Subspace method
DMC	dimethyl carbonate
DOD	Department of Defense
DPD-RX	Reactive Dissipative Particle Dynamics
DSM	distributed shared memory
EC	ethylene carbonate

E-DFT	embedded-DFT
EDL	electric double layer
EE-DFT	Exactly Embedded DFT
EM	energetic material
EMRM	Enterprise for Multiscale Research of Materials
EOS	equation of state
EPIC	Elastic Plastic Impact Computation code developed by Southwest Research Institute
FCC	face-centered cubic
FE	finite element
FED3	Finite Elements for Discrete Dislocation Dynamics
FEM	finite element method
FOX-7	1,1-diamino-2,2-dinitroethylene
GaN	gallium nitride
GPR	Gaussian process regression
HCP	hexagonal close-packed
HMS	hierarchical multiscale simulation
HOMO	highest occupied molecular orbital
HPC	high-performance computing
HPCMP	High Performance Computing Modernization Program
HYPRE	library of high-performance preconditioners and solvers featuring multigrid methods for the solution of large, sparse linear systems of equations on massively parallel computers
IE	ionization energy
JIT	just in time
KAIN	Krylov subspace Accelerated Inexact Newton method
KS	Kohn–Sham
LAMMPS	Large-scale Atomic/Molecular Massively Parallel Simulator
Li	lithium
LLNL	Lawrence Livermore National Laboratory

LS-DYNA	advanced general-purpose multiphysics simulation software package
LUMO	lowest unoccupied molecular orbital
MD	molecular dynamics
Mg	magnesium
ML	machine learning
MLDM	machine-learned delta model
MM	molecular modeling
MPI	standardized and portable message-passing standard designed to function on parallel computing architectures
MPMD	multiple-program-multiple-data
MUMPS	Multifrontal Massively Parallel Solver, for large sparse systems of linear algebraic equations on distributed memory parallel computers
NASA	National Aeronautics and Space Administration
NVE	isochoric-isoenergetic ensemble
NVT	isothermal-isochoric ensemble
OpenMP	application programming interface that supports multi-platform shared-memory multiprocessing programming
ParaDiS	Parallel Dislocation Simulator
PBE	a generalized gradient approximation functional for the exchange-correlation energy
PDL	prismatic dislocation loops
PE	polyethylene
PET	HPCMP User Productivity Enhancement and Training Program
PETN	pentaerythritol tetranitrate
QC-DFT	quasi-continuum DFT
QM	quantum mechanics
QMMS	quantum mechanics for material science
RCB	rechargeable calcium battery
RDX	1,3,5-*s*-triazine
ReaxFF	reactive bond order-based force field

RMB	rechargeable magnesium battery
RT	real time
SCF	self-consistent field
S	sulfur
SEI	solid electrolyte interphase
Sierra	Sandia National Laboratory's engineering mechanics simulation code suite
SOA	state of the art
STEX	scaled thermal explosion experiment
TATB	triamino trinitrobenzene
TC2	second-order trace conserving method
TD-DFT	time-dependent DFT
Ti	titanium
TINKER-HP	massively parallel classical molecular dynamics software suite that uses advanced polarizable force fields
TRS4	fourth-order trace resetting method
UQPy	uncertainty quantification package
VASP	Vienna Ab initio Simulation Package
VUMAT	vectorized user material
WiSE	water-in-salt
XL-BOMD	extended Lagrangian-BOMD
Zn	zinc

1 (PDF) DEFENSE TECHNICAL INFORMATION CTR DTIC OCA

1 (PDF) DEVCOM ARL
FCDD RLD DCI
TECH LIB

1 (PDF) DA HQ
DASA(R&T)

9 (PDF) USARMY AFC
L BROUSSEAU
J REGO
A LINZ
K WADE
S BRADY
J REGO
T KELLY
E JOSEPH
B SESSLER

2 (PDF) DEVCOM HQ
FCDD ST
C SAMMS
M HUBBARD

79 (PDF) DEVCOM ARL
FCDD RLC
C BEDELL
B SADLER
B PIEKARSKI
H EVERITT
FCDD RLC CA
L KAPLAN
FCDD RLC EM
J KNAP
KW LEITER
JC CRONE
FCDD RLC ES
G VIDEEN
S HILL
Y PAN
FCDD RLC I
B MACCALL
FCDD RLC N
BM RIVERA
A SWAMI
FCDD RLD
P BAKER
A KOTT
K JACOBS
FCDD RLD D
T ROSENBERGER
FCDD RLD E
KS FOSTER
FCDD RLD F
K KAPPRA
FCDD RLD FR
M TSCHOPP
FCDD RLD SM
L BLUM
FCDD RLH
J CHEN
PJ FRANASZCZUK
C LANE
K MCDOWELL
FCDD RLH B
JJ SUMNER
FCDD RLH F
JR GASTON
FCDD RLH T
D STRATIS-CULLUM
FCDD RLL
T KINES
FCDD RLL D
J S ADAMS
FCDD RLL DP
J MCCLURE
FCDD RLR
B HALPERN
S LEE
D STEPP
FCDD RLR E
RA MANTZ
C VARANASI
FCDD RLR EL
JX QIU
MD ULRICH
FCDD RLR EN
RA ANTHENIEN JR
FCDD RLR IC
MA FIELDS
SP IYER
FCDD RLR IM
JD MYERS
FCDD RLR IN
XN WANG
FCDD RLR
P REYNOLDS
FCDD RLR P
LL TROYER
FCDD RLR PC
D POREE
FCDD RLR PL
MK STRAND
FCDD RLS
J ALEXANDER
M GOVONI

M WRABACK
FCDD RLS C
M REED
FCDD RLS CC
S BEDAIR
FCDD RLS CE
O BORODIN
TR JOW
K XU
FCDD RLS CL
M DUBINSKIY
FCDD RLS E
RD DELROSARIO
FCDD RLS ED
K JONES
FCDD RLS EA
A ZAGHLOUL
FCDD RLS S
WL BENARD
FCDD RLS SO
W ZHOU
FCDD RLW
S KARNA
JF NEWILL
AM RAWLETT
SE SCHOENFELD
J ZABINSKI
FCDD RLW B
R BECKER
FCDD RLW M
ES CHIN
FCDD RLW MC
BC RINDERSPACHER
FCDD RLW S
V CHAMPAGNE
AL WEST
FCDD RLW T
RZ FRANCART
FCDD RLW TC
JD CLAYTON
FCDD RLW W
TV SHEPPARD
FCDD RLW WA
B RICE
R PESCE-RODRIGUEZ
WD MATTSON
FCDD RLW M
A HALL